Heliyon 8 (2022) e10176

Contents lists available at ScienceDirect

Heliyon

journal homepage: www.cell.com/heliyon

Research article

# Effect of additional $Fe^{2+}$ salt on electrocoagulation process for the degradation of methyl orange dye: An optimization and kinetic study

Sonia Akter, Md. Shahinoor Islam *

*Department of Chemical Engineering, Bangladesh University of Engineering and Technology, Dhaka, 1000, Bangladesh*

## HIGHLIGHTS

- EC represents limiting treatment performance for higher contaminant concentrations.
- 0.20 mmol.$L^{-1}$ $Fe^{2+}$ salt enhances the EC treatment performance of MO dye to 100%.
- EC followed first-order kinetic model, whereas $Fe^{2+}$ added EC followed second-order kinetic model.
- Operating cost was reduced to \$0.327 $m^{-3}$ from \$0.598 $m^{-3}$ for EC with additional $Fe^{2+}$.
- 58% COD was removed for 0.15 mmol.$L^{-1}$ $Fe^{2+}$ added EC for real textile wastewater.

## GRAPHICAL ABSTRACT

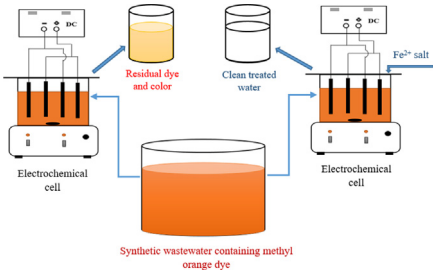


## ARTICLE INFO

*Keywords:*
Electrocoagulation
Iron electrodes
Cost estimation
Degradation kinetics
Methyl orange

## ABSTRACT

The wastewater generated from textile industries is highly colored and contains dyes including azo dyes, which are toxic to human and water-living organisms. The treatment of these azo dyes using conventional treatment techniques is challenging due to their recalcitrant properties. In the current study, the effect of additional $Fe^{2+}$ on electrocoagulation (EC) using Fe electrodes has been studied for the removal of methyl orange (MO) azo dye. pH between 4-5 was found to be optimum for EC and treatment efficiency decreased with increasing dye concentrations. With the addition of $Fe^{2+}$ salt, dye removal for a certain concentration was increased with the increase of current density and $Fe^{2+}$ up to a certain limit and after that, the removal efficiency decreased. The COD, color and dye removals were 88.5%, 93.1% and 100%, respectively, for EC of 200 mg.$L^{-1}$ dye solution using only 0.20 mmol.$L^{-1}$ $Fe^{2+}$ for 0.40 mA $cm^{-2}$ current density, whereas for EC, the respective removal efficiencies were 76.7%, 63.4% and 82.4% for 32 min. The respective operating cost for EC was \$768 $kg^{-1}$ removed dye (\$0.342 $m^{-3}$), whereas, for EC with additional $Fe^{2+}$ salt, it was \$350 $kg^{-1}$ removed dye (\$0.189 $m^{-3}$). The kinetic results revealed that the first-order kinetic model was fitted best for EC, whereas the second-order kinetic model was best fitted for $Fe^{2+}$ added EC. For real textile wastewater, 57.6% COD removal was obtained for 0.15 mmol.$L^{-1}$ $Fe^{2+}$ added EC compared to 27.8% COD removal for EC for 32 min. Based on the study we can conclude that $Fe^{2+}$ assisted EC can be used for effective treatment of textile wastewater containing toxic compounds like azo dyes.

* Corresponding author.
*E-mail address:* shahinoorislam@che.buet.ac.bd (Md.S. Islam).

https://doi.org/10.1016/j.heliyon.2022.e10176
Received 19 February 2022; Received in revised form 29 April 2022; Accepted 29 July 2022

## 1. Introduction

Textile industries, one of the significant economic contributors in developing countries like China, Vietnam, Bangladesh, India, Sri Lanka, etc., are identified as the largest source of water pollution (Holkar et al., 2016; Lellis et al., 2019). It has been reported that 1 kg of textile product generates 100–200 L of wastewater (Al-Mamun et al., 2021a) which contains both inorganic and organic substances such as metals, dyes, surfactants and microfibers (Yaseen and Scholz, 2019). Approximately 60–70% of the synthetic dyes used in textile processing units are azo dyes that are used due to the stability and fastness of the fabric (Benkhaya et al., 2020; Fernández-Fernández et al., 2013) and 10–15% of these synthetic dyes are lost in the effluent (Al-Mamun et al., 2019). These dyes are toxic to aquatic organisms, have poor biodegradability, and cause changes in the biological cycles of aquatic life adversely when mixed with surface water (Lellis et al., 2019). Due to higher volume, most textile industries discharge the effluent into nearby surface water bodies after inadequate treatment leaving an adverse influence on freshwater supplies and public health.

Physical, chemical and biological treatment technologies have been employed for textile wastewater treatment and a few treatment techniques for textile wastewaters are listed in Table 1. From Table 1, it can be seen that real textile wastewaters contain higher pollutants levels as compared to synthetic textile wastewater. However, physical processes like adsorption and filtration only separate contaminants with higher treatment costs (Couto et al., 2018; Pourrezaei et al., 2010; Roy et al., 2022), biological processes are inefficient (Dogan et al., 2020; Tiwari et al., 2017; Wesley et al., 2011) and chemical processes cause an intensification of dissolved components, costly and ineffective (Panizza and Cerisola, 2009). Advanced oxidation processes (AOPs) such as ozonation (Kurade et al., 2012; Wang et al., 2005), persulfate oxidation (Shuchi et al., 2021), UV/$H_2O_2$ (Al-Mamun et al., 2021b), solar-$TiO_2$ (Al-Mamun et al., 2022; Hasan Khan Neon and Islam, 2019) have become more popular for the treatment of textile dyes, but these processes cause higher treatment cost. Therefore, an efficient, affordable and environmentally friendly treatment technique is urgently required to treat and manage textile wastewaters for reuse and recycle purposes.

Electrocoagulation (EC) has been proved as a simple, reliable, less cost-oriented and efficient treatment technique for textile effluent (Akter et al., 2022; Khandegar and Saroha, 2013). In this process, on-site in-situ generated metallic ions by the electrolytic dissolution of the sacrificial anodes such as iron (Fe) and aluminum (Al) initiate the coagulation process (Camcioglu et al., 2017; Hakizimana et al., 2017; Shokri, 2018). Hybrid electrodes (Cletus et al., 2022; Sorayyaei et al., 2021), as well as electrodes with different designs (Wu et al., 2021) have also been applied for more efficient treatment of different textile dyes. In the current study, Fe electrodes were used due to their higher treatment efficiency, longer durability, lower cost and non-toxic nature than Al electrodes (Ghalwa et al., 2016; Ghernaout et al., 2011; Moreno et al., 2009). Also, Al electrodes eliminate contaminants only by EC mechanism whereas, Fe electrodes remove contaminants by both EC and electro-oxidation (EO) mechanisms (Benekos et al., 2019; Nasrullah et al., 2018). The anodic electrochemical reactions of Fe follow two mechanisms and generate $Fe(OH)_3$ and $Fe(OH)_2$ (Table 2) (Ghernaout, 2018; Mollah et al., 2001; Zodi et al., 2009). Gomes et al. (2007) observed that both $Fe^{2+}$ and $Fe^{3+}$ ions along with their organometallic complexes are present in the solution (Kamaraj and Vasudevan, 2015; Song et al., 2017). Additionally, the generated $Fe^{2+}$ gets oxidized into $Fe^{3+}$ in the reaction medium (Sasson et al., 2009). Researchers have also reported that $Fe^{3+}$ behaves as a stronger coagulant than $Fe^{2+}$ due to its higher destabilization power (Garcia-Segura et al., 2017; Linares-Hernández et al., 2009).

The generated ions ($Fe^{2+}$ and $Fe^{3+}$) in the solution can eliminate the pollutants by (i) involving chemical reaction with organics followed by precipitation, and (ii) producing agglomerates of colloidal particles followed by sequential removal of agglomerated flocs through flotation, which is assisted by the evolution of generated $H_2$ (Sahu et al., 2014; Suhan et al., 2021). For the removal of malathion pesticides by EC, Sankar and Sivasubramanian (2021) observed charge neutralization followed by sweep coagulation with the metal hydroxide to be the main removal mechanism. Elnakar and Buchanan (2020) also recommended that the in-situ generated ferric hydroxide acts as an adsorbent that removes the sCOD through chemisorption. Several phenomena like metal ion formation, electrochemical decomposition, hydrolysis, metal-organic attraction, etc., also happen concurrently during the pollutants' migration through the electric field. These might cause the separation of organic pollutants by altering both the physical and chemical properties of the pollutants (Canizares et al., 2007; Garcia-Segura et al., 2017; Sahu et al., 2014). Researchers recommended that the leading pollutant removal mechanisms depend on pollutant types and the operating principles of EC (Chen, 2004; Islam, 2019).

A comparatively smaller quantity of sludge is generated in EC compared to chemical coagulation (CC) and the typical uses of sludge are (i) manufacturing of fire brick after mixing with clay, (ii) application as fuel in boilers and incinerators, (iii) application of pyrolyzed sludge ash as additives in the clinker for cement manufacturing, and (iv) application of pyrolyzed sludge ash as adsorbents for wastewater treatment (Heikal, 2000; Islam et al., 2021; Kushwaha et al., 2010). Sankar and Sivasubramanian (2021) applied the sludge generated from EC of malathion pesticide for soil amendment and observed an extreme improvement in the quality and the geotechnical properties of the soil, making the sludge a minor threat to the environment.

EC treatment technique has some drawbacks like electrode passivation, higher electric energy consumption and generation of secondary pollutants (Al-Qodah et al., 2020), and lower amount of coagulant generation by the sacrificial anodes (Barrera Díaz and González-Rivas, 2015), which limit its applications and effectiveness. Researchers have recommended that the addition of coagulants into the electrochemical cell can enhance treatment efficiency (El-Ashtoukhy et al., 2017). With this concept, $FeSO_4.7H_2O$ salt was selected as the source of $Fe^{2+}$ that works as both a reducing agent (oxidation of $Fe^{2+}$ into $Fe^{3+}$) and coagulant.

In this study, degradation of methyl orange (MO) azo dye (anionic) using a customized EC reactor was investigated. MO ($C_{14}H_{14}N_3NaO_3S$, molecular weight: 327.34 g $mol^{-1}$, $\lambda_{max}$: 463 nm) (Yan et al., 2010) was selected due to its versatile use in textile industries, paints, cosmetics and laboratories (Ma et al., 2007; Ramírez et al., 2013; Schlichter et al., 2017; Zhang et al., 2012). Although several degradation techniques have been studied for MO, to the best of our knowledge, no previous study has elucidated the influence of additional $Fe^{2+}$ on the EC technique for MO dye degradation.

The main objective of this study was to investigate the influence of additional $Fe^{2+}$ on the EC treatment process using Fe electrodes for MO dye removal. The effects of pH, current density and initial dye concentrations as well as concentration of additional $Fe^{2+}$ were studied. EC process with and without additional $Fe^{2+}$ was also analyzed and compared using first-order, second-order and pseudo-second-order models to investigate the removal kinetics. Finally, EC with and without additional $Fe^{2+}$ salt was applied for the treatment of real textile wastewater to represent the applicability of EC in practice.

## 2. Materials and methods

### 2.1. Reagents

MO (ACS reagent, 85% purity) dye was purchased from Sigma-Aldrich (USA). Iron (II) sulfate heptahydrate ($FeSO_4.7H_2O$), was extra pure and was purchased from Scharlau (Spain). Potassium dichromate ($K_2Cr_2O_7$), mercuric sulfate ($HgSO_4$) and silver sulfate ($Ag_2SO_4$), used for the preparation of digestion solutions for COD measurement, were also purchased from Scharlau (Spain). Dilute (40%) sulfuric acid ($H_2SO_4$) and dilute (40%) sodium hydroxide (NaOH) were used for pH adjustment. All MO dye solutions were prepared with distilled water obtained from the laboratory supply.

**Table 1.** Textile wastewater treatment using different techniques.

| Type of pollutant | Treatment technology | Initial pollutant concentration | Experimental conditions | Results | References |
|---|---|---|---|---|---|
| Real textile wastewater | Sequential Chemical coagulation (CC)-Electro-Oxidation (EO) | pH: 9.3<br>Cond: 4010 $\mu$ S $cm^{-1}$<br>Turbidity (NTU): 161<br>COD: 720 $mg.L^{-1}$<br>TOC: 164 $mg.L^{-1}$<br>$BOD_5$: 115 $mg.L^{-1}$ | CC<br>$Al_2(SO_4)_3 \cdot 18H_2O$: 600 $mg.L^{-1}$ pH: 9.3<br>EO pH: 5.6<br>Cond: 4.7 mS $cm^{-1}$<br>Current density: 15 mA $cm^{-2}$<br>Electrode: BDD anode and Fe cathode<br>Time: 45 min | Color: 100%<br>COD: 93.5%<br>TOC: 75%<br>Cost: 6.91 USD/$m^3$ | GilPavas et al. (2018) |
| Real textile wastewater | CuO activated carbon (AC) composite with additonal peroxydisulfate (PDS) | COD: 450 $mg.L^{-1}$<br>BOD: 190 $mg.L^{-1}$<br>TOC: 213 $mg.L^{-1}$<br>Color (ADMI): 1209<br>TDS: 650 $mg.L^{-1}$<br>$Cl^-$: 122 $mg.L^{-1}$ pH: 7.6<br>Cu: 0.08 $mg.L^{-1}$ | PDS: 7 $mmol.L^{-1}$<br>CuO-AC: 1 $g.L^{-1}$ pH: 7<br>Time: 60 min | TOC: 61 %<br>Color: 95 %<br>COD: 72 %<br>BOD: 70 % | Kiani et al. (2020) |
| Real textile wastewater | Combined Chemical coagulation (CC), electrocoagulation (EC), and adsorption | $BOD_5$: 278.54 ± 65.23 $mg.L^{-1}$<br>COD: 1,346.17 ± 123.36 $mg.L^{-1}$<br>TSS: 178.28 ± 23.82 $mg.L^{-1}$ | Poly aluminum chloride (PAC) as coagulant,<br>Al electrodes for EC,<br>Pistachio nut shell ash as adsorbent | COD: 98% $BOD_5$: 94.2%<br>Dye: 99.9% | Bazrafshan et al. (2016) |
| Real textile wastewater | Advanced oxidation processes (AOPs) based on zero-valent aluminium (ZVAl) | pH: 7.10–7.80<br>COD: 2155 $mg.L^{-1}$<br>BOD: 500 $mg.L^{-1}$<br>Ammoniacal nitrogen: 699 $mg.L^{-1}$<br>$Cl^-$: 1463 $mg.L^{-1}$<br>TDS: 5190 $mg.L^{-1}$<br>TSS: 513 $mg.L^{-1}$ | ZVAl: 1 $g.L^{-1}$<br>$Fe^{3+}$: 0.5 $g.L^{-1}$<br>$H_2O_2$: 6.7 $g.L^{-1}$<br>Time: 3 h | COD: 97.9%<br>Color: 94.4%<br>Ammoniacal nitrogen: 58.3% | Khatri et al. (2018) |
| Real textile wastewater | $TiO_2$/UV | pH: 10.8<br>Temp: 31.2 °C<br>Cond: 13.6 mS $cm^{-1}$<br>TSS: <3 $mg.L^{-1}$<br>DOC: 382 $mg.L^{-1}$<br>COD: 1020 $mg.L^{-1}$<br>$BOD_5$: 110 $mg.L^{-1}$<br>$BOD_5$/COD: 0.11<br>$Cl^-$: 4578 $mg.L^{-1}$<br>Total nitrogen: 32.4 $mg.L^{-1}$ | pH: 4.5<br>$TiO_2$: 200 $mg.L^{-1}$<br>Radiation: 190 $kJ_{UV}.L^{-1}$ | DOC: 36% | Vilar et al. (2011) |
| | $H_2O_2$+$TiO_2$/UV | | pH: 4.5<br>$TiO_2$: 200 $mg.L^{-1}$<br>Radiation: 100 $kJ_{UV}.L^{-1}$<br>$H_2O_2$: 208.1 $mmol.L^{-1}$ | DOC: 90% | |
| | Solar-photo-Fenton | | $Fe^{2+}$: 100 $mg.L^{-1}$<br>Radiation: 49.1 $kJ_{UV}.L^{-1}$<br>$H_2O_2$: 203.2 $mmol.L^{-1}$ | DOC: 89% | |
| Synthetic wastewater containing Remazol Black B (RBB) | Electrocoagulation (EC) | RBB: 100 $mg.L^{-1}$<br>Starch: 1500 $mg.L^{-1}$<br>Glucose: 500 $mg.L^{-1}$<br>$Na_2CO_3$: 1000 $mg.L^{-1}$<br>$NaHCO_3$: 1000 $mg.L^{-1}$<br>NaOH: 500 $mg.L^{-1}$<br>NaCl: 1500 $mg.L^{-1}$ | pH: 3<br>Current density: 10 mA $cm^{-2}$<br>Time: 50 min<br>Electrode: SS | Color: 91% Dye: 86.5%<br>Turbidity: 60.4% COD: 19.8% | Suhan et al. (2020) |
| Real textile wastewater (Pre-treated) | Electrocoagulation (EC) | COD: 287 $mg.L^{-1}$<br>TOC: 240 $mg.L^{-1}$<br>Turbidity (NTU): 25<br>Cond: 7.6 ms $cm^{-1}$ pH: 8<br>TSS: 34 $mg.L^{-1}$<br>Cr: 0.028 $mg.L^{-1}$<br>Zn: 0.09 $mg.L^{-1}$<br>$Cl^-$: 0.1 mg. $L^{-1}$<br>Phenol: 0.355 mg. $L^{-1}$ | Time: 120 min pH: 5<br>Current density: 25 mA $cm^{-2}$<br>Electrode: Al | TOC: 42.5%<br>COD: 18.6%<br>Turbidity: 83.5%<br>SS: 64.7%<br>Color: 92% | Bener et al. (2019) |
| Textile industry wastewater | EC-Photo-Fenton (PF)-Adsorption | pH: 8.2<br>Cond: 5.04 mS $cm^{-1}$<br>Color (Pt–Co): 1399<br>BOD: 206 $mg.L^{-1}$<br>COD: 970 $mg.L^{-1}$<br>TOC: 220 $mg.L^{-1}$ | EC pH: 7<br>Current density: 10 mA $cm^{-2}$<br>Stirring: 60 rpm<br>Time: 10 min<br>PF pH: 4.3<br>$Fe^{2+}$: 1.1 $mmol.L^{-1}$<br>$H_2O_2$: 9.7 $mmol.L^{-1}$<br>Stirring: 100 rpm<br>Radiation: 365 nm<br>Time: 60 min<br>Adsorption<br>Granular activated carbon bed (Calgon Carbon, Pittsburgh, mesh 10) | Color: 100% COD: 76%<br>TOC: 78% Toxicity: 100% | GilPavas et al. (2019) |

(*continued on next page*)

**Table 1** (*continued*)

| Type of pollutant | Treatment technology | Initial pollutant concentration | Experimental conditions | Results | References |
|---|---|---|---|---|---|
| Real textile wastewater | EC (Fe)-Nanofiltration<br>EC (Al)-Nanofiltration | Color (Pt–Co): 2100<br>COD: 2690 mg.L$^{-1}$<br>Turbidity (NTU): 1500<br>TDS: 7500 mg.L$^{-1}$<br>TSS: 280 mg.L$^{-1}$<br>Cond: 14.95 mS cm$^{-1}$ pH: 7.03 | d: 10 mm<br>Stirring: 200 rpm pH: 7<br>CD: 20 mA cm$^{-2}$<br>Membrane: NP010 NF | Color: 87.8%<br>COD: 77.6%<br>Turbidity: 99.9%<br>Color: 95.2%<br>COD: 81%<br>Turbidity: 99.7% | Tavangar et al. (2019) |
| Synthetic wastewater containing reactive dye (RR45) | Adsorption with Symphoricarpus albus modified with sodium diethyldithiocarbamate | 100 mg.L$^{-1}$ | Continuous flow rate: 1.0 mL min$^{-1}$<br>pH: 2<br>BET surface area: 0.043 m$^2$ g$^{-1}$ | Dye: 91.89%<br>Adsorption capacity: 6.22 $\times$ 10$^{-5}$ mol g$^{-1}$ | Kara et al. (2012) |
| Synthetic wastewater containing Acid orange 5 | EC process | 60 mg.L$^{-1}$ | pH: 7<br>Current density: 2 mA cm$^{-2}$<br>Time: 60 min | Dye: 99.3<br>COD: 85.5% | Shokri (2019) |
| Synthetic wastewater containing Acid red 14 (AR14) | Electro peroxone process | 400 mg.L$^{-1}$ | Current intensity: 0.7 A<br>pH: 10<br>Time: 30 min<br>$Na_2SO_4$: 0.1mol.L$^{-1}$<br>Ozone injection: 0.25 L min$^{-1}$<br>Electrode: Pt- carbon-PTFE electrode | Dye: 100%<br>COD: 69% | Shokri Karimi (2020) |

*Cond: conductivity, SS: suspended solid, TDS: total dissolved solid, TSS: total suspended solid, d: inter-electrode distance.

### 2.2. Electrocoagulation reactor

All the EC experiments were conducted in an open, undivided, square cell made of 5 mm PVC transparent sheet having a cross-section of 14.8 $\times$ 14.8 cm$^2$ with a volume of 4 L (Figure 1). All the experiments were conducted at ambient temperature (around 30 °*C*) and four Fe electrodes (SS304 sheet) having dimensions of 13 cm $\times$ 9 cm $\times$ 0.15 cm were used in a monopolar-parallel (MP-P) connection mode with a total surface area of 930 cm$^2$. This is due to the cost-effective nature of monopolar (MP) connection over bipolar (BP) connection for both organic and inorganic pollutants (Alimohammadi et al., 2017; Ghosh et al., 2008; Vasudevan et al., 2013). Before each experiment, all the electrodes were abraded with a steel scrubber followed by sequential washing with tap water and distilled water. The distance between two consecutive electrodes was 3.7 cm and all the experiments were conducted for 2.7 L of sample solution having an immersion of 75% of the total electrode surface area. All the experiments were conducted under a stirred condition of 150 rpm by using a magnetic stirrer and 'Dazheng DC Power Supply' converter having a capacity of 5 A and 33 V was used for the power supply.

### 2.3. Experimental

The influence of pH on EC was observed at first for suitable pH selection as it determines the solution conductivity, pollutant particle distribution, particle-particle interaction, types of hydrolyzed metal species and concentration of gas bubbles (Moussa et al., 2017; Naje et al., 2017; Sahu et al., 2014). pH was optimized from experiments containing freshly prepared 100 mg.L$^{-1}$ dye solutions having initial pH in between 4-5 (acidic), 6–7 (neutral) and 8–9 (basic) under a constant current density of 0.11 mA cm$^{-2}$. At the optimum pH, the influence of variable dye concentrations on EC treatment performance was also investigated at 0.11 mA cm$^{-2}$ current density for 100, 200, and 300 mg.L$^{-1}$ dye solutions. Additionally, optimum current densities for 100, 200, and 300 mg.L$^{-1}$ dye solutions were determined at the optimum pH. In literature, it is mentioned that the dye concentration in textile wastewater ranged from 10 to 500 mg.L$^{-1}$ (Yaseen and Scholz, 2019). Therefore, the experiments were conducted for higher dye concentrations (100–300 mg.L$^{-1}$ MO dye).

The influence of additional $Fe^{2+}$ salt was explored for the removal of 200 mg.L$^{-1}$ MO solution at the optimum pH obtained from EC experiments. Also, the salt solution was added to a previously adjusted acidic solution under rapid mixing conditions to avoid the precipitation of $Fe^{2+}$ at higher pH (Pétrier et al., 2010). Optimum parameters were also evaluated for EC with additional $Fe^{2+}$ salt to compare with conventional EC treatment performances. Furthermore, both EC with and without additional $Fe^{2+}$ salt was investigated for the treatment of real textile wastewater collected from a local textile industry. The raw textile

**Table 2.** Reaction mechanisms for the dissolution of Fe electrodes.

| Mechanism 1: | Mechanism 2: |
|---|---|
| Anode:<br>$4Fe_{(s)} \rightarrow 4Fe^{2+}_{(aq)} + 8e^-$ (1)<br>$4Fe^{2+}_{(aq)} + 10\,H_2O_{(l)} + O_{2(g)} \rightarrow 4Fe(OH)_{3(s)} + 8H^+_{(aq)}$ (2)<br>Cathode:<br>$8H^+_{(aq)} + 8e^- \rightarrow 4H_{2(g)}$ (3)<br>Overall:<br>$4Fe_{(s)} + 10H_2O_{(l)} + O_{2(g)} \rightarrow 4Fe(OH)_{3(s)} + 4H_{2(g)}$ (4) | Anode:<br>$Fe_{(s)} \rightarrow Fe^{2+}_{(aq)} + 2e^-$ (5)<br>$Fe^{2+}_{(aq)} + 2OH^-_{(aq)} \rightarrow Fe(OH)_{2(s)}$ (6)<br>Cathode:<br>$2H_2O_{(l)} + 2e^- \rightarrow H_{2(g)} + 2OH^-_{(aq)}$ (7)<br>Overall:<br>$Fe_{(s)} + 2H_2O_{(l)} \rightarrow Fe(OH)_{2(s)} + H_{2(g)}$ (8) |

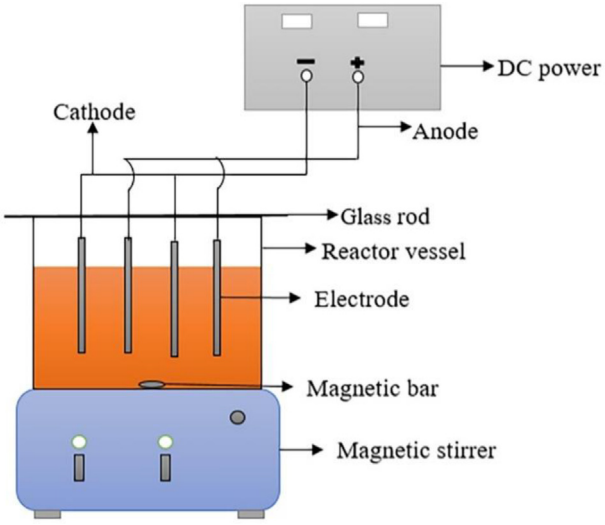


**Figure 1.** Schematic diagram of electrocoagulation reactor.

**Table 3.** Treatment performance and cost analysis of EC.

| | Dye conc. ($mg.L^{-1}$) | pH | Current density ($mA.cm^{-2}$) | % COD removal | % Color removal | % Dye removal | Cost analysis* | | | |
|---|---|---|---|---|---|---|---|---|---|---|
| | | | | | | | $C_{energy}$ ($kWh.m^{-3}$) × $10^3$ | $C_{metal}$ ($kg.m^{-3}$) × $10^3$ | OC ($/$m^3$) × $10^3$ | OC/kg removed dye ($/kg dye) |
| Optimization of pH | 100 | 4–5 | 0.11 | 66.7 | 91.1 | 96.6 | 152.1 | 36.8 | 54.8 | 231.7 |
| | | 6–7 | | 51.2 | 41.3 | 57.4 | 1123.5 | 36.0 | 164.7 | 1062.7 |
| | | 8–9 | | 35.7 | 36.1 | 40.2 | 604.9 | 36.0 | 105.6 | 972.8 |
| Optimization of current density | 100 | 4–5 | 0.11 | 66.7 | 91.1 | 96.6 | 152.1 | 36.8 | 54.8 | 231.7 |
| | | | 0.25 | 91.7 | 94.8 | 98.3 | 956.4 | 83.7 | 194.2 | 731.6 |
| | | | 0.32 | 78.2 | 85.4 | 91.3 | 1409.4 | 107.2 | 269.7 | 1093.9 |
| | | | 0.37 | 74.2 | 76.4 | 91.3 | 1932.9 | 123.9 | 346.4 | 1405.1 |
| | | | 0.40 | 75.3 | 63.7 | 79.1 | 3253.4 | 134.0 | 507.1 | 2374.5 |
| | 200 | 4–5 | 0.11 | 54.7 | 63.2 | 64.7 | 162.7 | 36.8 | 56.0 | 160.3 |
| | | | 0.25 | 61.2 | 85.2 | 83.3 | 1474.8 | 83.7 | 253.3 | 563.1 |
| | | | 0.32 | 91.2 | 88.1 | 96.3 | 2520.4 | 107.2 | 396.3 | 762.1 |
| | | | 0.37 | 71.3 | 78.5 | 87.8 | 3598.2 | 123.9 | 536.2 | 1131.0 |
| | | | 0.40 | 84.6 | 71.2 | 89.6 | 4050.7 | 134.0 | 598.0 | 1236.0 |
| | 300 | 4–5 | 0.11 | 43.2 | 52.6 | 57.6 | 191.0 | 36.8 | 59.2 | 127.0 |
| | | | 0.30 | 69.4 | 91.5 | 74.2 | 2227.9 | 100.5 | 356.2 | 592.6 |
| | | | 0.35 | 93.9 | 93.1 | 96.1 | 3004.2 | 117.2 | 461.7 | 593.1 |
| | | | 0.37 | 77.1 | 84.1 | 91.4 | 3735.0 | 123.9 | 551.8 | 745.3 |
| | | | 0.40 | 63.7 | 77.3 | 71.6 | 4243.6 | 134.0 | 620.0 | 1069.1 |

* Basis: 1 $m^3$ wastewater and 56 min treatment time; unit cost of energy (a): $0.114/kWh, unit cost of Fe electrode material (b): $1.017/kg (Kobya et al., 2016).

wastewater was highly polluted (pH: 9.5; total suspended solids, TSS: 1320 $mg.L^{-1}$; chemical oxygen demand, COD: 683 $mg.L^{-1}$; biological oxygen demand, $BOD_5$: 543 $mg.L^{-1}$). To evaluate the treatment performance and to compare with synthetic MO solution treatment, % COD removal was considered here.

### 2.4. Analytical procedures and instruments

For the assessment of treatment performance, samples were collected at a time interval of 8 min during operation and COD ($mg.L^{-1}$), color (Pt–Co) and dye concentrations ($mg.L^{-1}$) were measured. The sample solutions were filtered using a 0.2 $\mu$ m nylon syringe filter to eliminate the iron interference in COD measurement. 'HACH DR 6000' spectrophotometer was used for the measurement of color and absorbance of the sample solutions and COD of the digested samples. The color was measured based on a visible region of the spectrum and absorbance was measured based on maximum absorbance for each solution pH. Maximum absorbance for each solution pH was measured at first. pH indicator paper was used for pH measurement and hence, solution pH was expressed as pH range. Glass square cuvette was used for color and absorbance (320–1400 nm) measurement. For COD measurement, 'APHA 5220D' (closed reflux, colorimetric method) was used for the digestion of sample solutions. Unknown dye concentrations of the solutions were measured by using a calibration curve. % COD removal, % color removal and % dye removal were calculated to evaluate the treatment performance using Eq. (1) (Kader et al., 2022):

$$\%\ \text{removal} = \frac{C_o - C}{C_o} \times 100\% \quad (1)$$

where, $C_o$ and C are the initial and present values of the COD ($mg.L^{-1}$), color (Pt–Co) and dye concentrations ($mg.L^{-1}$), respectively.

The energy consumption per unit of dye removal (E) was calculated to compare the removal performances at different conditions using the following formula (Eq. 2):

$$E\left(\frac{KWh}{kg\ removed\ dye}\right) = \frac{I \times U \times t}{C_{MO} \times X \times V \times 10^3} \quad (2)$$

where I is the current intensity (A), U is the cell voltage (V), t is the treatment time (h), V is the volume of solution (L), $C_{MO}$ is the initial dye concentration ($mg.L^{-1}$) and X is the fraction removal for the treatment time.

### 2.5. Cost analysis

The applicability of a treatment technique depends both on treatment efficiency and cost-effectiveness. The operating cost (OC) of EC and $Fe^{2+}$ salt-assisted EC was calculated to evaluate the cost-effectiveness. OC of EC includes the cost of electrodes and energy consumption cost mainly (Kobya et al., 2011) and can be expressed by Eq. (3) (Kobya et al., 2016).

$$OC = a\ C_{energy} + b\ C_{electrode} \quad (3)$$

where, $C_{energy}$ is the energy consumption per unit volume ($kWh.m^{-3}$), $C_{electrode}$ is the amount of electrode consumption per unit volume ($kg.m^{-3}$), and a and b are unit cost of energy ($\$.kW^{-1}.h^{-1}$) and electrode material ($\$.kg^{-1}$), respectively. Value of unit cost of energy (a) was taken as \$0.114 $kW^{-1}\ h^{-1}$ and unit cost of Fe electrode material (b) was taken as \$1.017 $kg^{-1}$ (Kobya et al., 2016).

Formulae for $C_{energy}$ and $C_{electrode}$ calculation are expressed by Eqs. (4) and (5), respectively (Kobya et al., 2016):

$$C_{energy} = \frac{U \times i \times t_{EC}}{v \times 1000} \quad (4)$$

$$C_{electrode} = \frac{i \times t_{EC} \times M_{Fe} \times 3600}{z \times F \times v \times 1000} \quad (5)$$

where U is the applied voltage (V), i is the applied current (A), $t_{EC}$ is the EC treatment time (h), v is the solution volume ($m^3$), $M_{Fe}$ is the molecular weight of the Fe electrode (55.85 g $mol^{-1}$), z is the number of electrons involved in the oxidation/reduction reaction (z = 2) and F is the Faraday's constant (96,500 C $mol^{-1}$).

In the case of EC with additional $Fe^{2+}$ salt, the cost of added salt should also be added along with the cost of electricity consumption and metal dissolution and can be expressed by Eq. (6)

$$OC' = a\ C_{energy} + b\ C_{electrode} + c\ C_{salt} \quad (6)$$

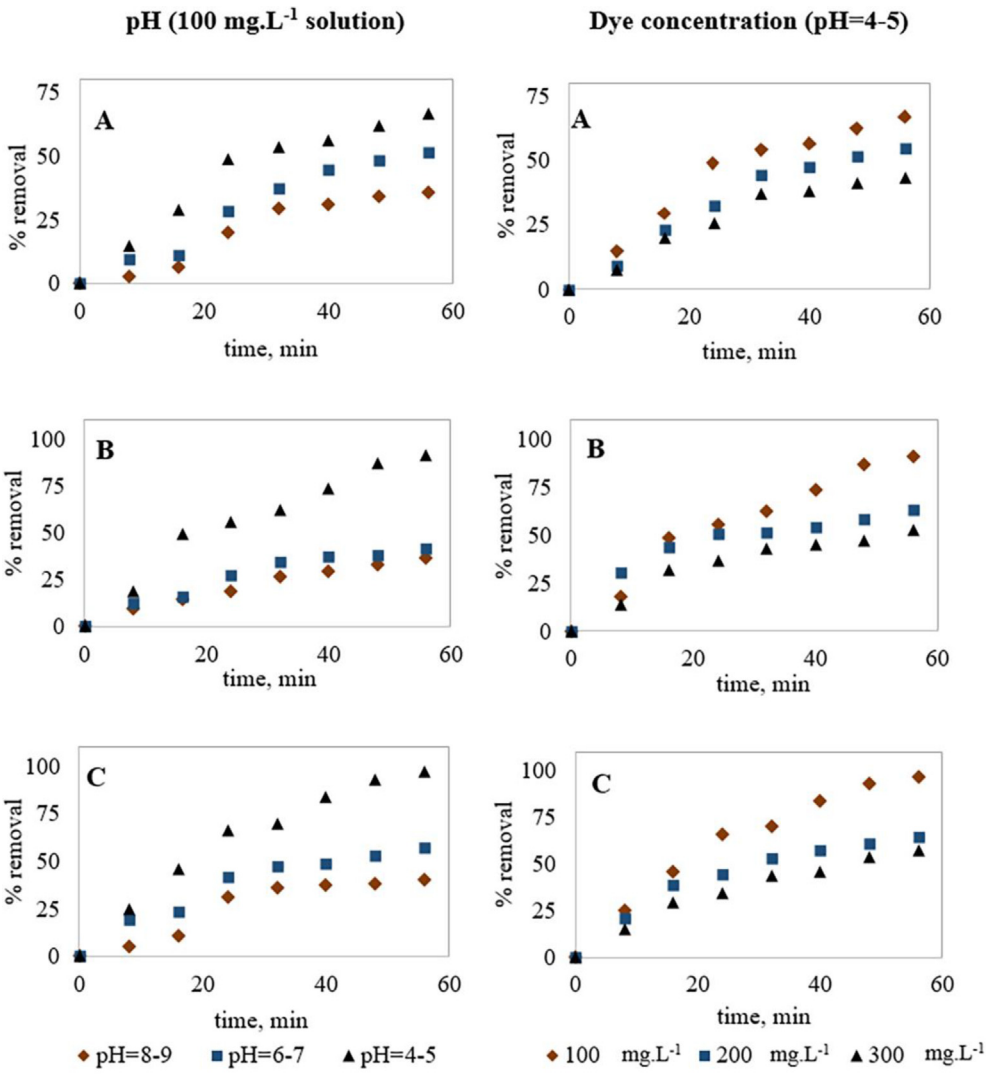


**Figure 2.** Effect of pH and dye concentrations on EC treatment efficiency; (A) %COD removal, (B) %Color removal and (C) %Dye removal (Note: current density was kept constant at 0.11 mA $cm^{-2}$).

where $C_{salt}$ is the quantity of salt per unit volume ($kg.m^{-3}$) and c is the unit cost of $FeSO_4.7H_2O$ that was taken as $\$8.8 \times 10^{-2}\ kg^{-1}$ (Suhan et al., 2020).

Additionally, the operating cost per unit of dye removal ($\$.kg^{-1}$ dye) was also calculated to evaluate the cost for pollutant removal using Eq. (7):

$$E\left(\frac{\$}{kg\ removed\ dye}\right) = \frac{TOC}{C_{MO} \times X \times V} \tag{7}$$

where TOC is the total operating cost ($), V is the volume of solution (L), $C_{MO}$ is the initial dye concentration ($kg.L^{-1}$) and X is the fraction removal for the treatment time.

### 2.6. Degradation kinetics

The degradation kinetics of 200 $mg.L^{-1}$ MO dye removal by EC and $Fe^{2+}$ assisted EC around the optimum current densities were studied using first-order, second-order and pseudo-second-order kinetic models for optimum treatment time. Eqs. (8), (9), and (10) represent the linearized first-order (Connors, 1990), second-order (Connors, 1990) and pseudo-second-order (Elkacmi et al., 2017) models, respectively.

$$\ln C = \ln C_0 - kt \tag{8}$$

$$\frac{1}{C} = kt + \frac{1}{C_0} \tag{9}$$

$$\frac{t}{C} = \frac{1}{kC_e^2} + \frac{t}{C_e} \tag{10}$$

where $C_o$ is the initial dye concentration ($mg.L^{-1}$), C is the dye concentration at any time ($mg.L^{-1}$), $C_e$ is the amount of pollutant removed at equilibrium ($mg.L^{-1}$) and k is the reaction rate constant.

## 3. Results and discussions

### 3.1. Influence of pH on EC

The pH optimization of an EC treatment process depends on electrode material and pollutant types (Koparal et al., 2008). Since solution pH governs the electrode dissolution and formation of hydrolyzed metal species in electrolyte media (Garcia-Segura et al., 2017; Katal and Pahlavanzadeh, 2011), pH was optimized for the EC treatment first. Experimental results are summarized in Table 3 and Figure 2. After 56 min,

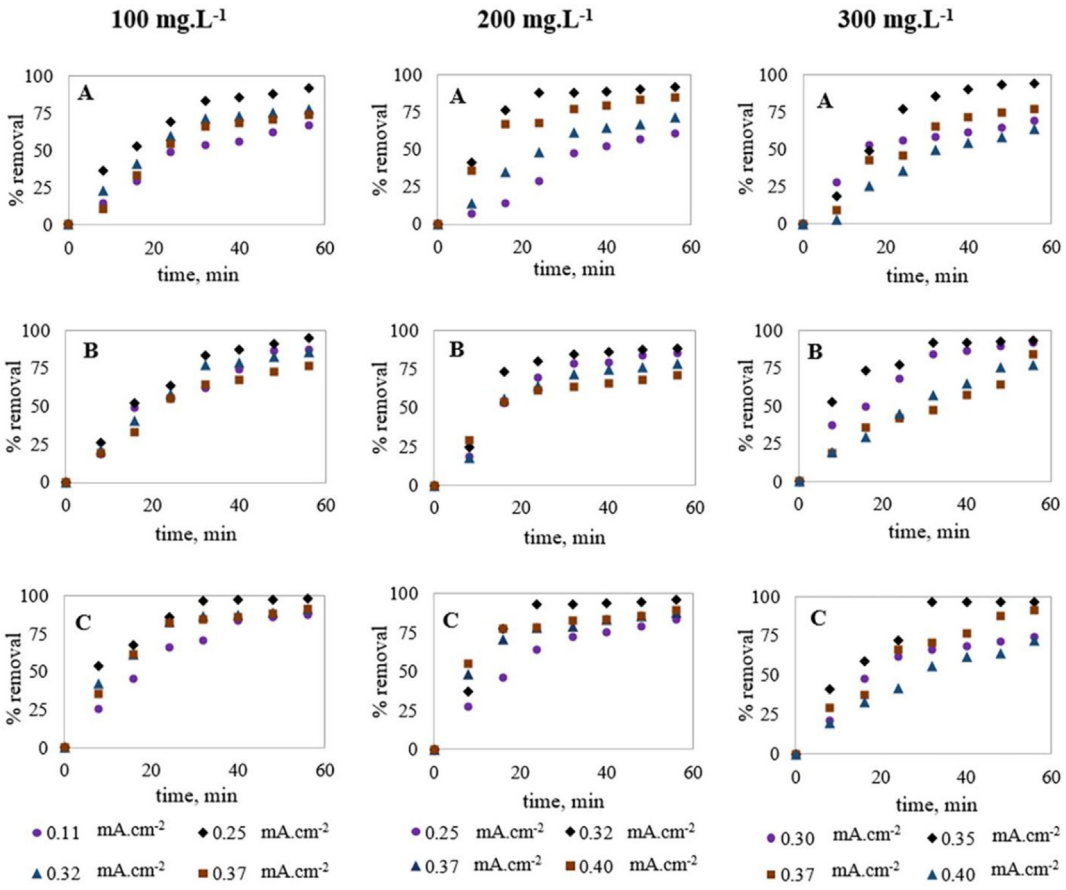


**Figure 3.** Optimization of EC for variable dye concentrations; (A) %COD removal, (B) %Color removal and (C) %Dye removal (Note: pH was kept between 4 to 5).

COD, color and dye removals for the acidic condition were 66.7%, 91.1% and 96.6%, respectively, whereas for the neutral condition these removals were 51.2%, 41.3% and 57.4%, respectively and for basic condition, these were 35.7%, 36.1% and 40.2%, respectively. Therefore, acidic conditions (pH = 4–5) showed the highest treatment performance for EC of MO dye, which supports the previous studies (Li et al., 2014; Sha et al., 2016; Wang et al., 2015; Zhao et al., 2014). This is due to the higher availability of surface charge of generated metal ions at acidic conditions compared to neutral and basic conditions (Mohora et al., 2014), which results in a higher rate of coagulation. Also, the generated Fe ions get precipitated at higher pH (Devi et al., 2009). Pétrier et al. (2010) investigated the easy breakdown of the complex structure of MO under acidic conditions. Devi et al. (2009) also investigated acidic pH to be obvious for MO and observed no color removal at basic conditions. Ma et al. (2007) also obtained 100% color removal and 89.7% COD removal for MO dye by EC at an initial pH of 5.

During the EC experiment, the solution pH changed towards the neutral range (pH = 6–7) supporting the previous studies (Al Aji et al., 2012; Elabbas et al., 2016). This might be the consumption of generated hydroxyl ions that happened during EC, which changed pH to the neutral range (Aswathy et al., 2016; Elabbas et al., 2016). According to Barrera Díaz et al. (2003), $Fe(OH)_2$ is the predominant hydroxide for pH between 4-5 and both $Fe(OH)_2$ and $Fe(OH)_3$ exist in the pH range of 5–7. Also, the organic compounds dissociate into charged ions depending on the solution pH (Ghernaout, 2013).

Additionally, the associated energy consumption per unit of dye removal for acidic, neutral and basic pHs were 0.15, 1.12 and 6.05 $kWh.m^{-3}$, respectively. This implies the more conductive nature of acidic

**Table 4.** Treatment performance and cost analysis of EC with additional $Fe^{2+}$ salt.

| | Salt conc. (mM) | Current density ($mA.cm^{-2}$) | % COD removal | % Color removal | % Dye removal | Cost analysis* | | | | |
|---|---|---|---|---|---|---|---|---|---|---|
| | | | | | | $C_{energy}$ ($kWh.m^{-3}$) × $10^3$ | $C_{salt}$ ($kg.m^{-3}$) × $10^3$ | $C_{metal}$ ($kg.m^{-3}$) × $10^3$ | OC ($/$m^3$) × $10^3$ | OC/kg removed dye ($/kg dye) |
| Optimization of $Fe^{2+}$ salt conc. | 0.15 | 0.40 | 83.6 | 91.8 | 91.3 | 1928.9 | 41.7 | 134.0 | 359.8 | 678.5 |
| | 0.20 | | 84.5 | 97.5 | 98.2 | 1633.1 | 55.6 | 134.0 | 327.3 | 617.2 |
| | 0.25 | | 83.6 | 92.3 | 94.1 | 1221.6 | 69.5 | 134.0 | 281.6 | 531.1 |
| Optimization of current density | 0.20 | 0.37 | 88.5 | 93.4 | 96.4 | 898.1 | 55.6 | 123.9 | 233.3 | 448.2 |
| | | 0.40 | 84.5 | 97.5 | 98.2 | 1633.1 | 55.6 | 134.0 | 327.3 | 617.2 |
| | | 0.46 | 85.3 | 88.3 | 94.6 | 2218.2 | 55.6 | 154.1 | 414.4 | 811.3 |

* Basis: 1 $m^3$ wastewater and 56 min treatment time; unit cost of energy (a): $0.114/kWh, unit cost of Fe electrode material (b): $1.017/kg (Kobya et al., 2016), unit cost of $FeSO_4.7H_2O$ (c): $8.8 \times 10^{-2}.kg^{-1}$ (Suhan et al., 2020).

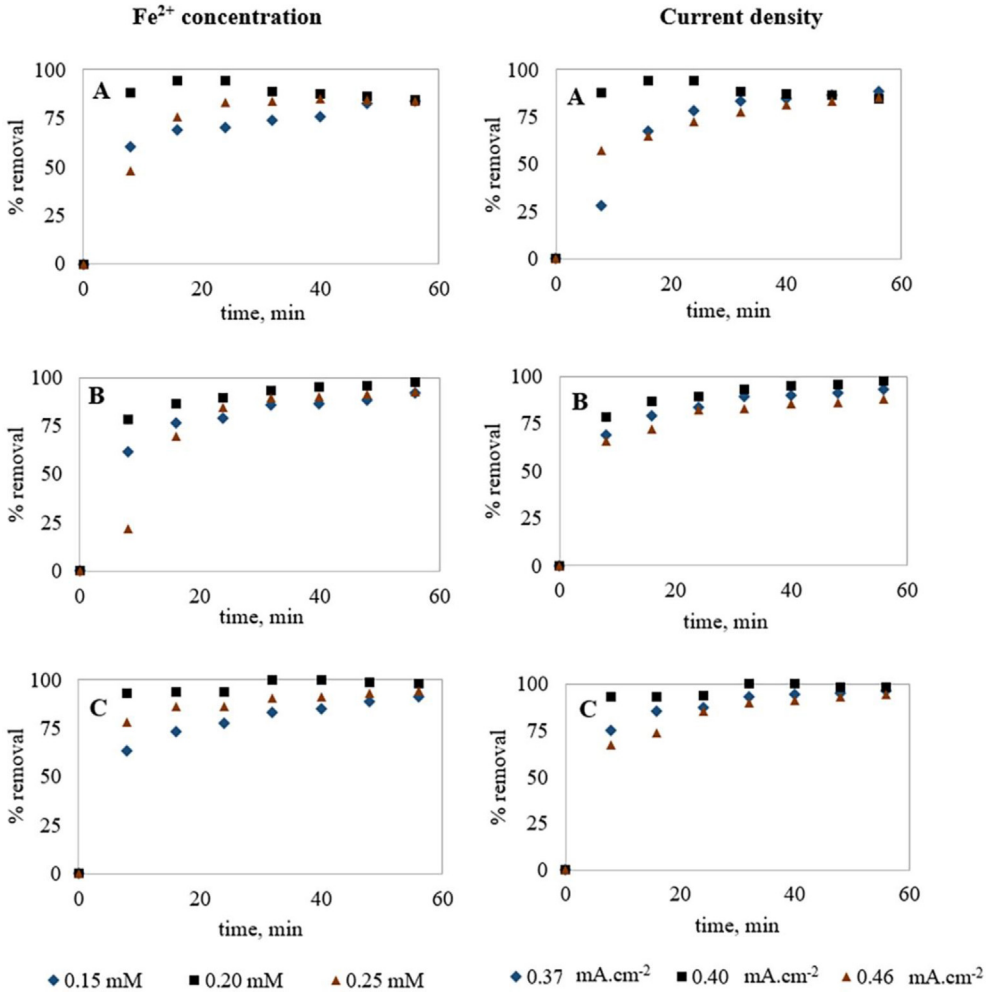


**Figure 4.** Optimization of EC with additional $Fe^{2+}$ salt for 200 mg.$L^{-1}$ dye solution treatment; (A) %COD removal, (B) %Color removal and (C) %Dye removal (Note: pH was kept between 4 to 5).

solution (due to $H^+$) and the least conductive nature at neutral pH. Finally, considering the issues of power requirement, treatment efficiency and higher corrosion rate of the electrodes in a more acidic solution, pH in the range of 4–5 was selected for the rest of the EC experiments.

### 3.2. Influence of variable dye concentrations on EC

Dye concentration varies extensively in textile wastewater and the treatment efficiency of EC depends on initial pollutant concentration (Yaseen and Scholz, 2019). To investigate the treatment performance for variable dye concentrations, several experiments were conducted for 100, 200 and 300 mg.$L^{-1}$ MO dye solutions at the optimized pH range (4–5) and at 0.11 mA $cm^{-2}$ current density. Treatment performances are summarized in Table 3 and removal trends are represented in Figure 2. After 56 min of treatment, COD removals for 100, 200 and 300 mg.$L^{-1}$ MO dye solutions were 66.7%, 54.6% and 43.2%, respectively; color removals were 91.1%, 63.2% and 52.6%, respectively and dye removals were 96.6%, 64.7% and 57.6%, respectively; indicating the highest removal efficiency for the lowest dye concentration (100 mg.$L^{-1}$). Additionally, removal efficiencies increased with increasing electrolysis time for 100 mg.$L^{-1}$ dye solution, whereas higher concentrations (200 and 300 mg.$L^{-1}$) showed limiting removal efficiencies, which were supported by previous studies (Benekos et al., 2019; El-Ashtoukhy et al., 2017; Zeboudji et al., 2013). Researchers recommended this effect due to the presence of insufficient amounts of flocs and exhaustion of adsorption capability of these limited flocs for higher contaminant concentrations (Ahmadzadeh et al., 2017; An et al., 2017; Kabdaşlı et al., 2012). Additionally, Fe(II) and Fe(III) ions generated for Fe electrodes also impose some color on the treated solution (Cañizares et al., 2007; Zaied et al., 2020), causing lower decolorization efficiency.

Additionally, associated energy consumption for the experiments containing 100, 200 and 300 mg.$L^{-1}$ MO dye solutions were 0.152, 0.163 and 0.191 kWh.$m^{-3}$, respectively. This power consumption implies higher energy consumption for solutions having higher contaminant concentrations. The power required and contaminant removal performance varied non-linearly with increasing pollutant concentrations, which is supported by previous studies (Ali et al., 2012; Hamdan and El-Naas, 2014). For the treatment of 25 and 55 mg.$L^{-1}$ synthetic MO dye in aqueous solutions, Irki et al. (2017) observed 86.89% and 73.81% of color removal was executed by the power consumptions of 31 and 33 kWh.$kg^{-1}$ MO dye, respectively.

### 3.3. Optimization of EC for variable dye concentrations

Current density has a collective effect on the EC process efficiency (Islam, 2019; Linares-Hernández et al., 2009) and optimum current density is required for effective treatment performance. Although a higher current density is required for a higher amount of metal coagulant generation for contaminant removal (Bayar et al., 2011; Farhadi et al., 2012), unnecessarily high current values may negatively affect the EC efficiency in addition to higher energy consumption (Farhadi et al., 2012;

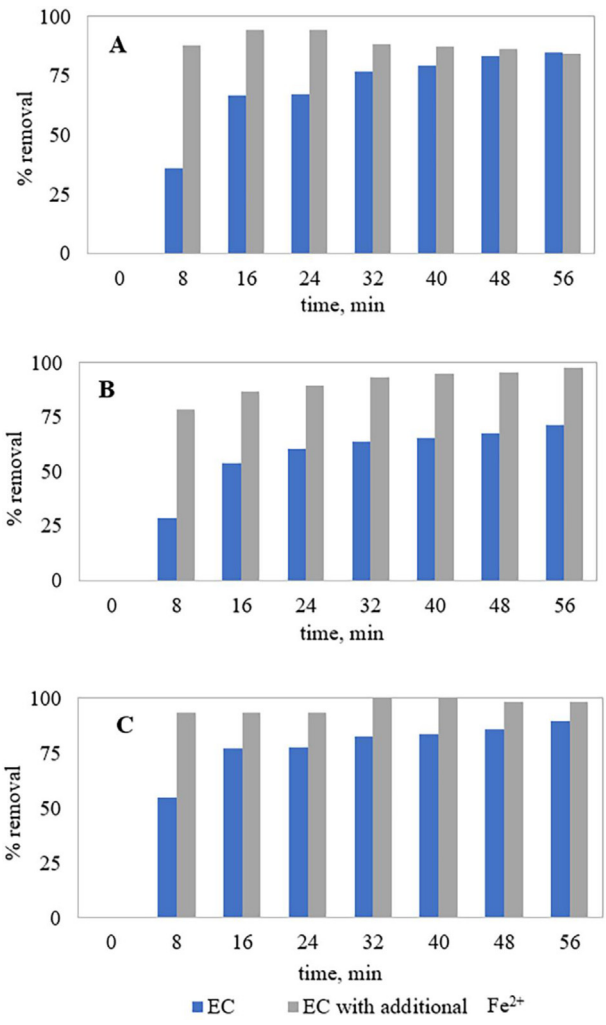


**Figure 5.** Competitive degradation of 200 mg.L$^{-1}$ MO solution by EC and EC with additional $Fe^{2+}$ salt at 0.40 mA cm$^{-2}$ current density; (A) %COD removal, (B) %Color removal and (C) %Dye removal.

Hakizimana et al., 2017). Also, Zaied et al. (2020) recommended that there is an optimum treatment time after which an increase in reaction time causes a slight increase in removal efficiency and higher energy consumption. EC for variable dye concentrations (100, 200 and 300 mg.L$^{-1}$) was optimized to observe the variation of these optimum parameters (current density and treatment time). With the concept of a higher amount of coagulant requirement for a higher amount of contaminant removal, higher current density was applied for higher dye concentrations and Table 3 and Figure 3 represent the results obtained in these experiments.

As seen (Figure 3), among all the experiments conducted for 100 mg.L$^{-1}$ MO solution, the experiment conducted at 0.25 mA cm$^{-2}$ current density showed the highest removal efficiency compared to other experiments and after 56 min, 91.7% COD, 94.8% color and 98.3% dye removals were observed. This indicates that the optimum current density for 100 mg.L$^{-1}$ MO dye solution treatment is 0.25 mA cm$^{-2}$. For the EC treatment of 200 mg.L$^{-1}$ MO, Figure 3 shows that the experiment conducted at 0.32 mA cm$^{-2}$ current density provided the highest removal efficiency compared to other experiments and after 56 min, 91.2% COD, 88.1% color and 96.3% dye removals were obtained. Current density below or above 0.32 mA cm$^{-2}$ showed lower treatment performance, indicating it as the optimum current density. Furthermore, 24 min was found to be the optimum treatment time for 200 mg.L$^{-1}$ dye degradation as no noticeable removal was obtained after this time. Similarly, for the EC treatment of 300 mg.L$^{-1}$ MO, 0.35 mA cm$^{-2}$ current density was found optimum and after 56 min, 93.9% COD, 93.1% color and 96.1% dye removals were obtained. Also, 30–35 min was observed as the optimum treatment time for 300 mg.L$^{-1}$ MO dye solution. From the above discussion, it can be concluded that both the optimum current density and optimum treatment time were increased with the increase of initial dye concentration, indicating a more coagulant requirement for higher dye concentrations. For the removal of organic pollutants by EC, researchers also recommended 10–30 min as the effective treatment time for a satisfactory removal (Benhadji et al., 2011; Espinoza-Quiñones et al., 2009; GilPavas et al., 2011).

### 3.4. Influence of different parameters on EC with additional $Fe^{2+}$

Although EC removes colloidal particles and suspended solids efficiently, it exhibits some difficulties for wastewaters having a large variety of pollutants (Akter et al., 2022). EC treatment for higher MO concentrations (Figure 2 and Figure 3) also represented limiting treatment performance and higher electrolysis time was required for satisfactory treatment performance. A combination of EC with other treatment techniques is recommended by several authors to achieve satisfactory treatment performance (Kabdaşlı et al., 2012; Shokri and Fard, 2022; Turan, 2020). With the objective to obtain satisfactory treatment performance, EC in combination with chemical coagulation (CC) was applied for MO dye solution treatment following other research studies (Bazrafshan et al., 2016; Shamaei et al., 2018). In this research, Fe salt ($FeSO_4.7H_2O$) was used in combination with EC treatment and the influence of salt concentration and current density on treatment performance were observed separately. Here, $Fe^{2+}$ acted as both a reducing agent (Sasson et al., 2009) and a coagulant while in the Fenton process, $Fe^{2+}$ acts as a catalyst for the generation of free radicals (de la Plata et al., 2008; Sun et al., 2009). Experimental results are summarized in Table 4 and removal trends are represented in Figure 4.

#### 3.4.1. Influence of salt ($Fe^{2+}$) concentration

As seen (Figure 4), among three experiments conducted at 0.40 mA cm$^{-2}$ current density having different salt concentrations (0.15, 0.20, and 0.25 mmol.L$^{-1}$), the experiment with 0.20 mmol.L$^{-1}$ $Fe^{2+}$ showed the highest removal efficiency and after 16 min, 94% COD removal, 85% color removal and 92% dye removal were obtained. Salt concentrations higher and lower than 0.20 mmol.L$^{-1}$ showed lower treatment performance. Besides, COD removal decreased after 24 min due to the increased concentration of $Fe^{2+}$ in the solution. This might be due to the overdosage of $Fe^{2+}$ that reversed the surface charge of particles, reducing the treatment efficiency (Farhadi et al., 2012; Hakizimana et al., 2017). For the degradation of MO by Advanced Fenton Process using zero valent metallic iron, Devi et al. (2009) reported that the excess concentration of $Fe^{2+}$ form hydroxide compound raising the pH of the solution, which further leads to precipitation, reducing the degradation rate.

Additionally, energy consumptions for the experiments containing 0.25, 0.20 and 0.15 mmol.L$^{-1}$ $Fe^{2+}$ were 1.22, 1.63 and 1.93 kWh.m$^{-3}$, respectively (for 56 min) implying increased solution conductivity with increasing salt concentration. Clearly, 0.20 mmol.L$^{-1}$ was the optimum $Fe^{2+}$ salt concentration and 20 min was the optimum treatment time for $Fe^{2+}$ added EC treatment of 200 mg.L$^{-1}$ MO dye solution at 0.40 mA cm$^{-2}$ current density. Previously, for electro-Fenton treatment, limits of $Fe^{2+}$ concentration were obtained in the range of 0.2–9.0 mmol.L$^{-1}$ (Pushpalatha and Krishna, 2017).

#### 3.4.2. Influence of current density

As both the electrode material and added salt was of Fe, the influence of current density on $Fe^{2+}$ salt added EC was observed for solutions containing 0.20 mmol.L$^{-1}$ $Fe^{2+}$. As seen (Figure 4), the experiment conducted at 0.40 mA cm$^{-2}$ current density showed the highest treatment performance and after 24 min, 94.1% COD removal, 88% color

**Table 5.** Different treatment processes for MO dye degradation.

| Treatment process | Initial pollutant levels | Treatment media/system specification | Operating conditions | Treatment efficiency | Reference |
|---|---|---|---|---|---|
| EC | 200 ppm MO | Monopolar SS electrode | pH:4-5<br>Time: 32 min<br>Volume: 2.7L | COD: 76.7%<br>Color: 63.4%<br>Dye: 82.4% | This study |
| $Fe^{2+}$ added EC | | | pH:4-5<br>Time: 24 min<br>Volume: 2.7L<br>$Fe^{2+}$: 0.20 mmol.$L^{-1}$ | COD: 94.1%<br>Color: 93.1%<br>Dye: 100% | This study |
| EC | Real textile wastewater<br>COD: 683 mg.$L^{-1}$ | Monopolar SS electrode | pH:4-5<br>Time: 56 min<br>Volume: 2.7L | COD: 35.4% | This study |
| $Fe^{2+}$ added EC | | | pH:4-5<br>Time: 32 min<br>Volume: 2.7L<br>Fe2+: 0.15 mmol.$L^{-1}$ | COD: 57.6% | This study |
| Catalytic degradation of MO | 10 mg.$L^{-1}$ | MCM-41-$NH_2$ | T: 30 °C pH: 6<br>Time: 120 min<br>Volume: 150 mL<br>$K_2S_2O_8$: 30 mg<br>Catalyst: 200 mg | Color: 35% | Schlichter et al. (2017) |
| | | Co/MCM-41-$NH_2$ | | Color: 96% | |
| | | Mn/MCM-41-$NH_2$ | | Color: 60% | |
| | | Cu/MCM-41-$NH_2$ | | Color: 98% | |
| | | SBA-15-$NH_2$ | | Color: 95% | |
| | | Cu/SBA-15-$NH_2$ | | Color: 96% | |
| | | Co/SBA-15-$NH_2$ | | Color: 100% | |
| MO dye degradation by EC | 125 mg.$L^{-1}$ | Periodic reversal of the electrodes (PREC) | pH: 7.4<br>Cond.: 9.4 mS $cm^{-1}$<br>Voltage: 4.4 V<br>Current density: 185 mA $cm^{-2}$<br>Time: 14 min<br>Cycle of periodic reversal of electrodes: 15 s | Color: 97%<br>Energy: 44 kWh/kg removed dye | Pi et al. (2014) |
| Microwave degradation of MO | 50 mg.$L^{-1}$ | $TiO_2$/AC/MW | pH: 6<br>Time: 1.5 min<br>Volume: 25 mL<br>Catalyst: 2.0 g.$L^{-1}$<br>Radiation:<br>750 W and 2450 MHz | Dye: 100% | Zhang et al. (2012) |
| MO degradation using $Zn^0$activated persulfate (PS) | 98 mg.$L^{-1}$ | | pH: 5<br>T: 25 °C<br>Time: 3 h<br>PS: 71 mg.$L^{-1}$<br>$Zn^0$: 1.3 g.$L^{-1}$ | COD: 85%<br>TOC: 58% | Li et al. (2014) |
| Microbial degradation of MO | 50 mg.$L^{-1}$ | Kocuria rosea (MTCC 1532) | pH: 6.5<br>T: 30 °C<br>Time: 75 min | Color: 95% | Parshetti et al. (2010) |
| MO degradation using Co nanoparticles | 100 mg.$L^{-1}$ | | pH: 2.5<br>Co nanoparticle: 0.5 g.$L^{-1}$<br>Time: 4 min<br>Stirring: 10 rpm | Color: 99% | Sha et al. (2016) |
| MO degradation by electro-catalytic oxidation | 400 mg.$L^{-1}$ | Double anode and single cathode system<br>Anode: Fe plate and graphite plate<br>Cathode: graphite plate<br>Cathode is assisted by $Co_2O_3$-CuO-$PO_4^{3-}$ modified kaolin | pH: 5<br>CD: 30 mA $cm^{-2}$<br>NaCl: 2.5 g.$L^{-1}$ d: 0.5 cm<br>Stirring: 100 rpm<br>Time: 60 min | Coloar: 100%<br>COD: 89.7% | Ma et al. (2007) |

Note: MCM-41 and SBA-16: metal supports, GO: graphene oxide, SSA: specific surface area, MF: magnetic field, EC: electrocoagulation, EO: electro-oxidation.

removal and 96% dye removal were obtained. Also, removal efficiency decreased after 24 min due to the increased concentration of $Fe^{2+}$ in the solution. Current density higher or lower than 0.40 mA $cm^{-2}$ showed lower treatment performance (Figure 4). Additionally, power consumption for the experiments conducted at 0.37, 0.40 and 0.46 mA $cm^{-2}$ current densities were 0.9, 1.6 and 2.2 kW h.$m^{-3}$, respectively (for 56 min) implying higher power consumption for higher current density. Clearly, for $Fe^{2+}$ added EC treatment of 200 mg.$L^{-1}$ MO dye solution using Fe electrodes, 0.40 mA $cm^{-2}$ was the optimum current density using 0.20 mmol.$L^{-1}$ $Fe^{2+}$ salt and 20 min were observed as the optimum treatment time.

### 3.5. Competitive treatment performance and power requirements

As the applicability of an EC process depends both on treatment performance and cost-efficiency, a competitive study was performed between EC with and without $Fe^{2+}$ salt addition for the treatment of 200 mg.$L^{-1}$ MO solution at 0.40 mA $cm^{-2}$ current density. As seen in Figure 5, EC with additional $Fe^{2+}$ (0.20 mmol.$L^{-1}$) showed higher removal performance compared to EC due to the collective effect of CC and EC. EC with additional $Fe^{2+}$ provided the highest COD removal efficiency for 24 min, whereas COD removal for EC increased with increasing treatment time. This was due to the over-dosage of $Fe^{2+}$ ions

**Table 6.** Modeling parameters for EC and $Fe^{2+}$ salt added EC of 200 ppm dye solution at different current density (Note: k = reaction rate constant).

| | Dye conc. (ppm) | pH | Current density ($mA.cm^{-2}$) | Parameters | First-order | Second-order | Pseudo second-order |
|---|---|---|---|---|---|---|---|
| EC | 200 | 4–5 | 0.25 | $r^2$ | 0.99 | 0.96 | 0.93 |
| | | | | k | 0.0405 | 0.0004 | -0.0043 |
| | | | 0.32 | $r^2$ | 0.96 | 0.88 | 0.87 |
| | | | | k | 0.0945 | 0.0024 | -0.013 |
| | | | 0.37 | $r^2$ | 0.92 | 0.96 | 0.97 |
| | | | | k | 0.0508 | 0.0007 | -0.0074 |
| EC with $Fe^{2+}$ salt | 200 | 4–5 | 0.37 | $r^2$ | 0.87 | 0.96 | 0.96 |
| | | | | k | 0.0897 | 0.0016 | -0.0153 |
| | | | 0.40 | $r^2$ | 0.66 | 0.67 | 0.99 |
| | | | | k | 0.1083 | 0.0031 | -0.0616 |
| | | | 0.46 | $r^2$ | 0.94 | 0.96 | 0.90 |
| | | | | k | 0.0753 | 0.0012 | -0.0102 |

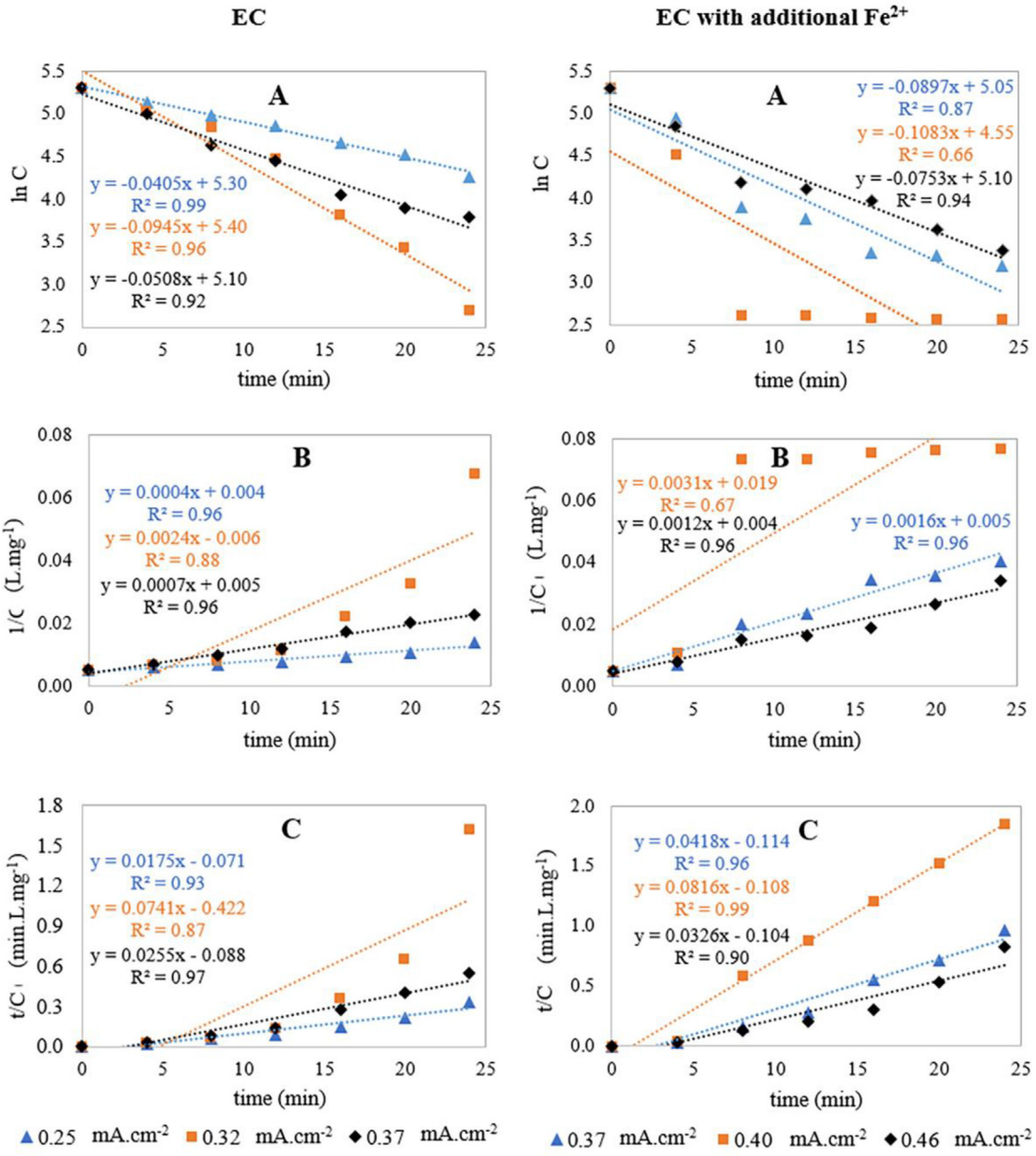


**Figure 6.** Kinetic model plots of EC and $Fe^{2+}$ salt added EC treatment for 200 $mg.L^{-1}$ MO dye at different current densities; (A) First-order model, (B) Second-order model, (C) Pseudo second-order model.

in solution after 24 min for EC with additional $Fe^{2+}$. Considering the COD, color and dye removal for $Fe^{2+}$ salt added EC compared to EC, 32 min could be considered for the highest removal performance. After 32 min, the treatment efficiency of $Fe^{2+}$ salt added EC (88.5% COD, 93.1% color and 100% dye) was much higher than for EC (76.7% COD, 63.4% color and 82.4% dye). Clearly, treatment performance for EC with additional $Fe^{2+}$ was more time-dependent compared to EC. Also, the power consumptions for EC and $Fe^{2+}$ added EC was 2.31 and 0.93 kWh.$m^{-3}$, respectively for 32 min. This implies that $Fe^{2+}$ added EC exhibited a lower power requirement with higher removal capability compared to EC only. From this comparison, it can be concluded that only a smaller amount of $Fe^{2+}$ salt can make the EC treatment process more feasible for industrial applications. Table 5 represents a comparison of MO dye removal from the current study with other research studies. As seen (Table 5), catalytic degradation and oxidation processes provided higher removal efficiencies compared to EC and $Fe^{2+}$ added EC. According to Pi et al. (2014), periodic reversal of the electrodes or application of AC current in EC or $Fe^{2+}$ added EC could improve COD removal.

Treatment performance of EC with and without $Fe^{2+}$ could also be improved by supplying air (oxygen) into the EC cell to increase the oxidation of $Fe^{2+}$ into $Fe^{3+}$ (Kumar et al., 2018). The limiting performance of this process could also be due to the passivation of Fe electrodes (Shamaei et al., 2018) which could be ignored by using AC current supply (Pi et al., 2014; Yang et al., 2015).

### 3.6. Cost analysis

The operating cost (OC) of EC experiments at variable conditions was calculated by using Eqs. (3), (4), and (5) and are summarized in Table 3. As seen (Table 3), the lowest OC was obtained for acidic pH ($0.055 $m^{-3}$, $232 $kg^{-1}$ removed dye) due to the lower energy consumption. OC for 100 mg.$L^{-1}$ dye solution at optimum condition (0.25 mA $cm^{-2}$) was found $0.194 $m^{-3}$ ($731.6 $kg^{-1}$ removed dye) that was higher than for the experiment conducted at 0.11 mA $cm^{-2}$ and lower than other experiments, but it (0.25 mA $cm^{-2}$) provided highest removal performance. Similarly, OC for 200 and 300 mg.$L^{-1}$ dye removal at optimum conditions were $0.396 $m^{-3}$ ($762 $kg^{-1}$ removed dye) and $0.462 $m^{-3}$ ($593 $kg^{-1}$ removed dye), respectively, showing increased OC for increasing dye concentration.

For EC with additional $Fe^{2+}$ salt, OC was calculated by using Eqs. (4), (5), and (6) and calculated results are summarized in Table 4. As seen, OC decreased with increasing salt concentration irrespective of the cost of added salt. This was due to the higher conductivity of solutions having higher salt concentration, lowering the power consumption. Furthermore, OC increased with increasing current density for a particular salt concentration. OC for the experiment having 0.20 mmol.$L^{-1}$ $Fe^{2+}$ and 0.40 mA $cm^{-2}$ current density was $0.327 $m^{-3}$ ($617 $kg^{-1}$ removed dye), whereas, for EC of 200 mg.$L^{-1}$ dye solution at 0.40 mA $cm^{-2}$ current density was $0.598 $m^{-3}$ ($1236 $kg^{-1}$ removed dye). This implies a higher removal capability of $Fe^{2+}$ added EC with lower OC as compared to conventional EC.

### 3.7. Kinetics of MO dye degradation

Kinetics of MO dye degradation was evaluated by comparing the values of regression coefficient and reaction rate constant (k). All the experiments were conducted at the same pH range (4–5) and kinetic studies were conducted for 24 min treatment time (optimum treatment time for 200 mg.$L^{-1}$ dye degradation) around the optimum current density. To represent the kinetic study using a more reliable data series, samples were collected at 4 min intervals. The computed results for first-order, second-order and pseudo-second-order kinetics are summarized in Table 6 and represented by Figure 6.

As seen, the degradation of MO by EC is more fitted to first-order kinetics ($r^2$ = 0.99, 0.96 and 0.92, respectively for 0.25, 0.32 and 0.37 mA $cm^{-2}$ current density). Also, a decrease in reaction rate constant (k) for current density higher and lower than 0.32 mA $cm^{-2}$ indicates this as the optimum current density. Degradation of MO by EC with additional $Fe^{2+}$ is more fitted to second-order kinetics ($r^2$ = 0.96, 0.67 and 0.96, respectively for 0.37, 0.40 and 0.46 mA $cm^{-2}$ current density). The highest value of reaction rate constant (k) at 0.40 mA $cm^{-2}$ current density (0.0031 L $mg^{-1}$.$min^{-1}$) implies maximum removal performance at this current density that was also found optimum. Poor regression coefficient for the experiment conducted at 0.40 mA $cm^{-2}$ might be due to the more instantaneous removal of dyes within the first few minutes (93% dye removal for 8 min) and slower removal of remaining dye molecules after a few minutes. Clearly, EC with and without additional $Fe^{2+}$ salt followed two different kinetic models for the removal of MO dye.

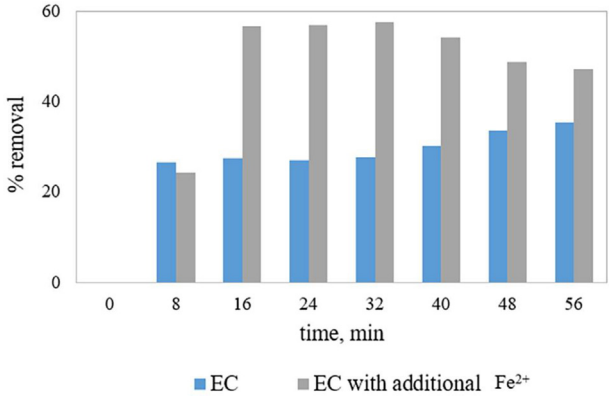


**Figure 7.** EC and $Fe^{2+}$ added EC for real wastewater treatment.

Pseudo-second-order kinetics was also studied for both EC and EC with additional $Fe^{2+}$ salt. The negative values of the reaction rate constant indicate a poor pseudo-second-order fit for MO dye removal by both EC and EC with additional $Fe^{2+}$ salt.

He et al. (2013) observed the degradation of 106 mg.$L^{-1}$ MO solution by the electro-Fenton (EC + $Fe^{2+}$+$H_2O_2$) process and the order of reaction was found 1.4164. For the photo-degradation of MO using a $TiO_2$--mercury lamp, Dai et al. (2007) also investigated that dye degradation followed second-order kinetics having a reaction rate constant of 4.234 $mol^{-1}$ $min^{-1}$.

### 3.8. Experiment with real textile wastewater

An experiment with real textile wastewater was conducted using both EC and $Fe^{2+}$ salt added EC. Both the experiments were conducted for 56 min. 0.15 mmol.$L^{-1}$ $Fe^{2+}$ salt concentration was used to observe the effect of additional $Fe^{2+}$ salt for real wastewater treatment and experimental results are represented by Figure 7. As seen, for the EC experiment, % COD removal increased with increasing treatment time and 35.4% COD removal was obtained after 56 min. EC with additional $Fe^{2+}$ showed more instantaneous COD removal performance and 57.6% COD removal was obtained after 32 min. After 32 min, COD removal decreased due to the accumulation of $Fe^{2+}$ in bulk solution, representing $Fe^{2+}$ added EC more time-dependent. Vidal et al. (2016) evaluated EC for real textile wastewater treatment and obtained 60% COD removal and 85% TOC removal at a pH of 4 using Al electrodes. From Table 1, it can be said that the combination of electro-oxidation with photo-degradation processes provides satisfactory treatment performance for real textile wastewater treatment. Hence, a combination of any photo-degradation technique with $Fe^{2+}$ added EC could improve the treatment performance for real textile wastewater.

## 4. Conclusion

Acidic pH (4–5) was found optimum for the removal of MO by EC. Also, treatment performance decreased with increasing dye

concentrations, and the optimum treatment time and current density were increased for higher dye concentrations. EC with additional $Fe^{2+}$ showed higher and more instantaneous removal efficiency with lower power consumption and lower operating cost (OC) compared to conventional EC. Under optimum conditions, 76.7% COD, 63.4% color and 82.4% dye removals were obtained for EC with an operating cost of \$0.342 $m^{-3}$ (\$768 $kg^{-1}$ removed dye), whereas 88.5% COD, 93.1% color and 100% dye removals were obtained for $Fe^{2+}$(0.20 mmol.$L^{-1}$) added EC with an operating cost of \$0.189 $m^{-3}$ (\$350 $kg^{-1}$ removed dye) for 32 min treatment time. Therefore, it can be concluded that EC with additional $Fe^{2+}$ salt is very efficient in terms of both treatment performance and operating cost.

## Declarations

### *Author contribution statement*

Sonia Akter: Conceived and designed the experiments; Performed the experiments; Analyzed and interpreted the data; Wrote the paper.

Md Shahinoor Islam: Conceived and designed the experiments; Contributed reagents, materials, analysis tools or data; Wrote the paper.

### *Funding statement*

Dr Md Shahinoor Islam was supported by Bangladesh University of Engineering and Technology [006].

### *Data availability statement*

No data was used for the research described in the article.

### *Declaration of interests statement*

The authors declare no conflict of interest.

### *Additional information*

No additional information is available for this paper.

## Acknowledgements

We are grateful to the Department of Chemical Engineering of Bangladesh University of Engineering and Technology (BUET) for providing laboratory facilities. We are also grateful to K. M. Nazmus Sakib (an undergraduate student, Department of Chemical Engineering, BUET) for assisting us in the laboratory.

## References

Ahmadzadeh, S., Asadipour, A., Pournamdari, M., Behnam, B., Rahimi, H.R., Dolatabadi, M., 2017. Removal of ciprofloxacin from hospital wastewater using electrocoagulation technique by aluminum electrode: optimization and modelling through response surface methodology. Process Saf. Environ. 109, 538–547.

Akter, S., Suhan, M.B.K., Islam, M.S., 2022. Recent advances and perspective of electrocoagulation in the treatment of wastewater: a review. Environ. Nanotechnol. Monit. Manag. 17, 100643.

Al Aji, B., Yavuz, Y., Koparal, A.S., 2012. Electrocoagulation of heavy metals containing model wastewater using monopolar iron electrodes. Separ. Purif. Technol. 86, 248–254.

Al-Mamun, M.R., Hossain, K.T., Mondal, S., Khatun, M.A., Islam, M.S., Khan, M.Z.H., 2022. Synthesis, characterization, and photocatalytic performance of methyl orange in aqueous $TiO_2$ suspension under UV and solar light irradiation. S. Afr. J. Chem. Eng. 40, 113–125.

Al-Mamun, M.R., Kader, S., Islam, M.S., Khan, M.Z.H., 2019. Photocatalytic activity improvement and application of UV-$TiO_2$ photocatalysis in textile wastewater treatment: a review. J. Environ. Chem. Eng. 7 (5), 103248.

Al-Mamun, M.,R., Karim, M.,N., Afroj, N., Kader, S., Islam, M.,S., Khan, M.Z.H., 2021a. Photocatalytic performance assessment of GO and Ag co-synthesized $TiO_2$ nanocomposite for the removal of methyl orange dye under solar irradiation. Environ. Technol. Innovat. 22, 101537.

Al-Mamun, M.R., Kader, S., Islam, M.S., 2021b. Solar-TiO2 immobilized photocatalytic reactors performance assessment in the degradation of methyl orange dye in aqueous solution. Environ. Nanotechnol. Monit. Manag. 16, 100514.

Al-Qodah, Z., Tawalbeh, M., Al-Shannag, M., Al-Anber, Z., Bani-Melhem, K., 2020. Combined electrocoagulation processes as a novel approach for enhanced pollutants removal: a state-of-the-art review. Sci. Total Environ. 744, 140806.

Ali, I., Khan, T.A., Asim, M., 2012. Removal of arsenate from groundwater by electrocoagulation method. Environ. Sci. Pollut. Res. 19 (5), 1668–1676.

Alimohammadi, M., Askari, M., Dehghani, M.H., Dalvand, A., Saeedi, R., Yetilmezsoy, K., Heibati, B., McKay, G., 2017. Elimination of natural organic matter by electrocoagulation using bipolar and monopolar arrangements of iron and aluminum electrodes. Int. J. Environ. Sci. Te. 14 (10), 2125–2134.

An, C., Huang, G., Yao, Y., Zhao, S., 2017. Emerging usage of electrocoagulation technology for oil removal from wastewater: a review. Sci. Total Environ. 579, 537–556.

Aswathy, P., Gandhimathi, R., Ramesh, S.T., Nidheesh, P.V., 2016. Removal of organics from bilge water by batch electrocoagulation process. Separ. Purif. Technol. 159, 108–115.

Barrera-Dıaz, C., Urena-Nunez, F., Campos, E., Palomar-Pardavé, M., Romero-Romo, M., 2003. A combined electrochemical-irradiation treatment of highly colored and polluted industrial wastewater. Radiat. Phys. Chem. 67 (5), 657–663.

Barrera Díaz, C.E., González-Rivas, N., 2015. The use of Al, Cu, and Fe in an integrated electrocoagulation-ozonation process. J. Chem. Neuroanat.

Bayar, S., Yıldız, Y.Ş., Yılmaz, A.E., İrdemez, Ş., 2011. The effect of stirring speed and current density on removal efficiency of poultry slaughterhouse wastewater by electrocoagulation method. Desalination 280 (1-3), 103–107.

Bazrafshan, E., Alipour, M.R., Mahvi, A.H., 2016. Textile wastewater treatment by application of combined chemical coagulation, electrocoagulation, and adsorption processes. Desalination Water Treat. 57 (20), 9203–9215.

Benekos, A.K., Zampeta, C., Argyriou, R., Economou, C.N., Triantaphyllidou, I.E., Tatoulis, T.I., Tekerlekopoulou, A.G., Vayenas, D.V., 2019. Treatment of table olive processing wastewaters using electrocoagulation in laboratory and pilot-scale reactors. Process Saf. Environ. Protect. 131, 38–47.

Bener, S., Bulca, Ö., Palas, B., Tekin, G., Atalay, S., Ersöz, G., 2019. Electrocoagulation process for the treatment of real textile wastewater: effect of operative conditions on the organic carbon removal and kinetic study. Process Saf. Environ. Protect. 129, 47–54.

Benhadji, A., Ahmed, M.T., Maachi, R., 2011. Electrocoagulation and effect of cathode materials on the removal of pollutants from tannery wastewater of Rouïba. Desalination 277 (1-3), 128–134.

Benkhaya, S., M'rabet, S., El Harfi, A., 2020. Classifications, properties, recent synthesis and applications of azo dyes. Heliyon 6 (1), 3271.

Camcioglu, S., Ozyurt, B., Hapoglu, H., 2017. Effect of process control on optimization of pulp and paper mill wastewater treatment by electrocoagulation. Process Saf. Environ. 111, 300–319.

Cañizares, P., Jiménez, C., Martínez, F., Saez, C., Rodrigo, M.A., 2007. Study of the electrocoagulation process using aluminum and iron electrodes. Ind. Eng. Chem. Res. 46 (19), 6189–6195.

Canizares, P., Martínez, F., Lobato, J., Rodrigo, M.A., 2007. Break-up of oil-in-water emulsions by electrochemical techniques. J. Hazard Mater. 145 (1-2), 233–240.

Chen, G., 2004. Electrochemical technologies in wastewater treatment. Separ. Purif. Technol. 38 (1), 11–41.

Cletus, A., Athira, S., Ramesh, A.G., Priya, K.L., Indu, M.S., 2022. Performance evaluation of electrocoagulation with hybrid electrodes in the decolourisation of methyl orange dye. In: Recent Advancements in Civil Engineering. Springer, Singapore, pp. 443–451.

Connors, K.A., 1990. Chemical Kinetics: the Study of Reaction Rates in Solution. Wiley-VCH Verlag GmbH.

Couto, C.F., Lange, L.C., Amaral, M.C.S., 2018. A critical review on membrane separation processes applied to remove pharmaceutically active compounds from water and wastewater. J. Water Proc. Eng. 26, 156–175.

Dai, K., Chen, H., Peng, T., Ke, D., Yi, H., 2007. Photocatalytic degradation of methyl orange in aqueous suspension of mesoporous titania nanoparticles. Chemosphere 69 (9), 1361–1367.

de la Plata, G.B.O., Alfano, O.M., Cassano, A.E., 2008. Optical properties of goethite catalyst for heterogeneous photo-Fenton reactions: comparison with a titanium dioxide catalyst. Chem. Eng. J. 137 (2), 396–410.

Devi, L.G., Kumar, S.G., Reddy, K.M., Munikrishnappa, C., 2009. Photo degradation of Methyl Orange an azo dye by Advanced Fenton Process using zero valent metallic iron: influence of various reaction parameters and its degradation mechanism. J. Hazard Mater. 164 (2-3), 459–467.

Dogan, A., Płotka-Wasylka, J., Kempińska-Kupczyk, D., Namieśnik, J., Kot-Wasik, A., 2020. Detection, identification and determination of chiral pharmaceutical residues in wastewater: problems and challenges. TrAC, Trends Anal. Chem. 122, 115710.

El-Ashtoukhy, E.Z., Amin, N.K., Abd El-Latif, M.M., Bassyouni, D.G., Hamad, H.A., 2017. New insights into the anodic oxidation and electrocoagulation using a self-gas stirred reactor: a comparative study for synthetic CI Reactive Violet 2 wastewater. J. Clean. Prod. 167, 432–446.

Elabbas, S., Ouazzani, N., Mandi, L., Berrekhis, F., Perdicakis, M., Pontvianne, S., Pons, M.N., Lapicque, F., Leclerc, J.P., 2016. Treatment of highly concentrated tannery wastewater using electrocoagulation: influence of the quality of aluminium used for the electrode. J. Hazard Mater. 319, 69–77.

Elkacmi, R., Kamil, N., Bennajah, M., 2017. Upgrading of Moroccan olive mill wastewater using electrocoagulation: kinetic study and process performance evaluation. J. Urban Environ. Eng. 11 (1), 30–41.

Elnakar, H., Buchanan, I., 2020. Soluble chemical oxygen demand removal from bypass wastewater using iron electrocoagulation. Sci. Total Environ. 706, 136076.

Espinoza-Quiñones, F.R., Fornari, M.M., Módenes, A.N., Palácio, S.M., Trigueros, D.E., Borba, F.H., Kroumov, A.D., 2009. Electrocoagulation efficiency of the tannery effluent treatment using aluminium electrodes. Water Sci. Technol. 60 (8), 2173–2185.
Farhadi, S., Aminzadeh, B., Torabian, A., Khatibikamal, V., Fard, M.A., 2012. Comparison of COD removal from pharmaceutical wastewater by electrocoagulation, photoelectrocoagulation, peroxi-electrocoagulation and peroxi-photoelectrocoagulation processes. J. Hazard Mater. 219, 35–42.
Fernández-Fernández, M., Sanromán, M.Á., Moldes, D., 2013. Recent developments and applications of immobilized laccase. Biotechnol. Adv. 31 (8), 1808–1825.
Garcia-Segura, S., Eiband, M.M.S., de Melo, J.V., Martínez-Huitle, C.A., 2017. Electrocoagulation and advanced electrocoagulation processes: a general review about the fundamentals, emerging applications and its association with other technologies. J. Electroanal. Chem. 801, 267–299.
Ghalwa, N.M.A., Saqer, A.M., Farhat, N.B., 2016. Removal of Reactive Red 24 dye by clean electrocoagulation process using iron and aluminum electrodes. J. Chem. Eng. Process Technol.
Ghernaout, D., 2013. Advanced oxidation phenomena in electrocoagulation process: a myth or a reality? Desalination Water Treat. 51 (40-42), 7536–7554.
Ghernaout, D., 2018. Electrocoagulation process: achievements and green perspectives. Colloid Surface Sci 3, 1–5.
Ghernaout, D., Ghernaout, B., Naceur, M.W., 2011. Embodying the chemical water treatment in the green chemistry—a review. Desalination 271 (1-3), 1–10.
Ghosh, D., Medhi, C.R., Purkait, M.K., 2008. Treatment of fluoride containing drinking water by electrocoagulation using monopolar and bipolar electrode connections. Chemosphere 73 (9), 1393–1400.
GilPavas, E., Dobrosz-Gómez, I., Gómez-García, M.Á., 2018. Optimization of sequential chemical coagulation-electro-oxidation process for the treatment of an industrial textile wastewater. J. Water Proc. Eng. 22, 73–79.
GilPavas, E., Dobrosz-Gómez, I., Gómez-García, M.Á., 2011. The removal of the trivalent chromium from the leather tannery wastewater: the optimisation of the electro-coagulation process parameters. Water Sci. Technol. 63 (3), 385–394.
GilPavas, E., Dobrosz-Gómez, I., Gómez-García, M.Á., 2019. Optimization and toxicity assessment of a combined electrocoagulation, H2O2/Fe2+/UV and activated carbon adsorption for textile wastewater treatment. Sci. Total Environ. 651, 551–560.
Gomes, J.A., Daida, P., Kesmez, M., Weir, M., Moreno, H., Parga, J.R., Irwin, G., McWhinney, H., Grady, T., Peterson, E., Cocke, D.L., 2007. Arsenic removal by electrocoagulation using combined Al–Fe electrode system and characterization of products. J. Hazard Mater. 139 (2), 220–231.
Hakizimana, J.N., Gourich, B., Chafi, M., Stiriba, Y., Vial, C., Drogui, P., Naja, J., 2017. Electrocoagulation process in water treatment: a review of electrocoagulation modeling approaches. Desalination 404, 1–21.
Hamdan, S.S., El-Naas, M.H., 2014. Characterization of the removal of Chromium (VI) from groundwater by electrocoagulation. J. Ind. Eng. Chem. 20 (5), 2775–2781.
Hasan Khan Neon, M., Islam, M.S., 2019. $MoO_3$ and Ag co-synthesized $TiO_2$ as a novel heterogeneous photocatalyst with enhanced visible-light-driven photocatalytic activity for methyl orange dye degradation. Environ. Nanotechnol. Monit. Manag. 12, 100244.
He, W., Yan, X., Ma, H., Yu, J., Wang, J., Huang, X., 2013. Degradation of methyl orange by electro-Fenton-like process in the presence of chloride ion. Desalination Water Treat. 51 (34-36), 6562–6571.
Heikal, M., 2000. Effect of temperature on the physico-mechanical and mineralogical properties of Homra pozzolanic cement pastes. Cement Concr. Res. 30 (11), 1835–1839.
Holkar, C.R., Jadhav, A.J., Pinjari, D.V., Mahamuni, N.M., Pandit, A.B., 2016. A critical review on textile wastewater treatments: possible approaches. J. Environ. Manag. 182, 351–366.
Irki, S., Ghernaout, D., Naceur, M.W., 2017. Decolourization of Methyl Orange (MO) by electrocoagulation (EC) using iron electrodes under a magnetic field (MF). Desalination Water Treat. 79, 368–377.
Islam, M.,S., Kwak, J.-H., Nzediegwu, C., Wang, S., Palansuriya, K., Kwon, E.,E., Anne Naeth, M., Gamal El-Din, M., Ok, Y.,S., Chang, S.X., 2021. Biochar heavy metal removal in aqueous solution depends on feedstock type and pyrolysis purging gas. Environ. Pollut. 281, 117094.
Islam, S.D.U., 2019. Electrocoagulation (EC) technology for wastewater treatment and pollutants removal. Sustain. Water Res. Manage. 5 (1), 359–380.
Kabdaşlı, I., Arslan-Alaton, I., Ölmez-Hancı, T., Tünay, O., 2012. Electrocoagulation applications for industrial wastewaters: a critical review. Environ. Technol. 1 (1), 2–45.
Kader, S., Al-Mamun, M.R., Suhan, M.B.K., Shuchi, S.B., Islam, M.S., 2022. Enhanced photodegradation of methyl orange dye under UV irradiation using MoO3 and Ag doped TiO2 photocatalysts. Environ. Technol. Innovat. 27, 102476.
Kamaraj, R., Vasudevan, S., 2015. Evaluation of electrocoagulation process for the removal of strontium and cesium from aqueous solution. Chem. Eng. Res. Des. 93, 522–530.
Kara, I., Akar, S.T., Akar, T., Ozcan, A., 2012. Dithiocarbamated Symphoricarpus albus as a potential biosorbent for a reactive dye. Chem. Eng. J. 211, 442–452.
Katal, R., Pahlavanzadeh, H., 2011. Influence of different combinations of aluminum and iron electrode on electrocoagulation efficiency: application to the treatment of paper mill wastewater. Desalination 265 (1-3), 199–205.
Khandegar, V., Saroha, A.K., 2013. Electrocoagulation for the treatment of textile industry effluent–a review. J. Environ. Manag. 128, 949–963.
Khatri, J., Nidheesh, P.V., Singh, T.A., Kumar, M.S., 2018. Advanced oxidation processes based on zero-valent aluminium for treating textile wastewater. Chem. Eng. J. 348, 67–73.
Kiani, R., Mirzaei, F., Ghanbari, F., Feizi, R., Mehdipour, F., 2020. Real textile wastewater treatment by a sulfate radicals-Advanced Oxidation Process: peroxydisulfate decomposition using copper oxide (CuO) supported onto activated carbon. J. Water Proc. Eng. 38, 101623.
Kobya, M., Demirbas, E., Ulu, F., 2016. Evaluation of operating parameters with respect to charge loading on the removal efficiency of arsenic from potable water by electrocoagulation. J. Environ. Chem. Eng. 4 (2), 1484–1494.
Kobya, M., Gebologlu, U., Ulu, F., Oncel, S., Demirbas, E., 2011. Removal of arsenic from drinking water by the electrocoagulation using Fe and Al electrodes. Electrochim. Acta 56 (14), 5060–5070.
Koparal, A.S., Yildiz, Y.Ş., Keskinler, B., Demircioğlu, N., 2008. Effect of initial pH on the removal of humic substances from wastewater by electrocoagulation. Separ. Purif. Technol. 59 (2), 175–182.
Kumar, A., Nidheesh, P.V., Kumar, M.S., 2018. Composite wastewater treatment by aerated electrocoagulation and modified peroxi-coagulation processes. Chemosphere 205, 587–593.
Kurade, M.B., Waghmode, T.R., Kagalkar, A.N., Govindwar, S.P., 2012. Decolorization of textile industry effluent containing disperse dye Scarlet RR by a newly developed bacterial-yeast consortium BL-GG. Chem. Eng. J. 184, 33–41.
Kushwaha, J.P., Srivastava, V.C., Mall, I.D., 2010. Organics removal from dairy wastewater by electrochemical treatment and residue disposal. Separ. Purif. Technol. 76 (2), 198–205.
Lellis, B., Fávaro-Polonio, C.Z., Pamphile, J.A., Polonio, J.C., 2019. Effects of textile dyes on health and the environment and bioremediation potential of living organisms. Biotechnol. Res. Innov. 3 (2), 275–290.
Li, H., Guo, J., Yang, L., Lan, Y., 2014. Degradation of methyl orange by sodium persulfate activated with zero-valent zinc. Separ. Purif. Technol. 132, 168–173.
Linares-Hernández, I., Barrera-Díaz, C., Roa-Morales, G., Bilyeu, B., Urena-Nunez, F., 2009. Influence of the anodic material on electrocoagulation performance. Chem. Eng. J. 148 (1), 97–105.
Ma, H., Wang, B., Luo, X., 2007. Studies on degradation of methyl orange wastewater by combined electrochemical process. J. Hazard Mater. 149 (2), 492–498.
Mohora, E., Rončević, S., Agbaba, J., Tubić, A., Mitić, M., Klašnja, M., Dalmacija, B., 2014. Removal of arsenic from groundwater rich in natural organic matter (NOM) by continuous electrocoagulation/flocculation (ECF). Separ. Purif. Technol. 136, 150–156.
Mollah, M.Y.A., Schennach, R., Parga, J.R., Cocke, D.L., 2001. Electrocoagulation (EC)-science and applications. J. Hazard Mater. 84 (1), 29–41.
Moreno C, H.A., Cocke, D.L., Gomes, J.A., Morkovsky, P., Parga, J.R., Peterson, E., Garcia, C., 2009. Electrochemical reactions for electrocoagulation using iron electrodes. Ind. Eng. Chem. Res. 48 (4), 2275–2282.
Moussa, D.T., El-Naas, M.H., Nasser, M., Al-Marri, M.J., 2017. A comprehensive review of electrocoagulation for water treatment: potentials and challenges. J. Environ. Manag. 186, 24–41.
Naje, A.S., Chelliapan, S., Zakaria, Z., Ajeel, M.A., Alaba, P.A., 2017. A review of electrocoagulation technology for the treatment of textile wastewater. Review. Chem. Eng-New York 33 (3), 263–292.
Nasrullah, M., Singh, L., Krishnan, S., Sakinah, M., Zularisam, A.W., 2018. Electrode design for electrochemical cell to treat palm oil mill effluent by electrocoagulation process. Environ. Technol. Innovat. 9, 323–341.
Panizza, M., Cerisola, G., 2009. Direct and mediated anodic oxidation of organic pollutants. Chem. Rev. 109 (12), 6541–6569.
Parshetti, G.K., Telke, A.A., Kalyani, D.C., Govindwar, S.P., 2010. Decolorization and detoxification of sulfonated azo dye methyl orange by Kocuria rosea MTCC 1532. J. Hazard Mater. 176 (1-3), 503–509.
Pétrier, C., Torres-Palma, R., Combet, E., Sarantakos, G., Baup, S., Pulgarin, C., 2010. Enhanced sonochemical degradation of bisphenol-A by bicarbonate ions. Ultrason. Sonochem. 17 (1), 111–115.
Pi, K.W., Xiao, Q., Zhang, H.Q., Xia, M., Gerson, A.R., 2014. Decolorization of synthetic methyl orange wastewater by electrocoagulation with periodic reversal of electrodes and optimization by RSM. Process Saf. Environ. 92 (6), 796–806.
Pourrezaei, P., Afzal, A., Ding, N., Islam, M.S., Moustafa, A., Drzewicz, P., Chelme-Ayala, P., Gamal El-Din, M., 2010. Physico-chemical processes. Water environment research. Lit. Rev. 82 (10), 997–1072.
Pushpalatha, M., Krishna, B.M., 2017. Electro-fenton process for waste water treatment. A review. Int. J. Adv. Res. Ideas Innov. Tech. 3 (1), 439–451.
Ramírez, Cecilia, Saldaña, Adriana, Hernández, Berenice, Acero, Roberto, Guerra, Ricardo, Garcia-Segura, Sergi, EnricBrillas, Juan, M., Peralta-Hernández, 2013. Electrochemical oxidation of methyl orange azo dye at pilot flow plant using BDD technology. J. Ind. Eng. Chem. 19 (2), 571–579.
Roy, H., Prantika, T.R., Riyad, M.H., Paul, S., Islam, M.S., 2022. Synthesis, characterizations and RSM analysis of *Citrus macroptera* peel derived biochar for textile dye treatment. S. Afr. J. Chem. Eng. 41, 129–139.
Sahu, O., Mazumdar, B., Chaudhari, P.K., 2014. Treatment of wastewater by electrocoagulation: a review. Environ. Sci. Pollut. Res. 21 (4), 2397–2413.
Sankar, M.R., Sivasubramanian, V., 2021. Optimization and evaluation of malathion removal by electrocoagulation process and sludge management. J. Environ. Chem. Eng. 9 (5), 106147.
Sasson, M.B., Calmano, W., Adin, A., 2009. Iron-oxidation processes in an electroflocculation (electrocoagulation) cell. J. Hazard Mater. 171 (1-3), 704–709.
Schlichter, S., Sapag, K., Dennehy, M., Alvarez, M., 2017. Metal-based mesoporous materials and their application as catalysts for the degradation of methyl orange azo dye. J. Environ. Chem. Eng. 5 (5), 5207–5214.
Sha, Y., Mathew, I., Cui, Q., Clay, M., Gao, F., Zhang, X.J., Gu, Z., 2016. Rapid degradation of azo dye methyl orange using hollow cobalt nanoparticles. Chemosphere 144, 1530–1535.

Shamaei, L., Khorshidi, B., Perdicakis, B., Sadrzadeh, M., 2018. Treatment of oil sands produced water using combined electrocoagulation and chemical coagulation techniques. Sci. Total Environ. 645, 560–572.
Shokri, A., 2018. Employing electrocoagulation for the removal of Acid Red 182 in aqueous environment by using Box-Behenken design method, Desalin. Water Treat. 115, 281–287.
Shokri, A., 2019. Application of electrocoagulation process for the removal of Acid orange 5 in synthetic wastewater. Iran. J. Chem. Chem. Eng. (IJCCE). 38 (2), 113–119.
Shokri, A., Fard, M.S., 2022. A critical review in electrocoagulation technology applied for oil removal in industrial wastewater. Chemosphere 288, 132355.
Shokri, A., Karimi, S., 2020. Treatment of aqueous solution containing acid red 14 using an electro peroxone process and a box-Behnken experimental design. Archive. Hygiene Sci. 9 (1), 48–57.
Shuchi, S.B., Suhan, M.B.K., Humayun, S.B., Haque, M.E., Islam, M.S., 2021. Heat-activated potassium persulfate treatment of Sudan Black B dye: degradation kinetic and thermodynamic studies. J. Water Proc. Eng. 39, 101690.
Song, P., Yang, Z., Zeng, G., Yang, X., Xu, H., Wang, L., Xu, R., Xiong, W., Ahmad, K., 2017. Electrocoagulation treatment of arsenic in wastewaters: a comprehensive review. Chem. Eng. J. 317, 707–725.
Sorayyaei, S., Raji, F., Rahbar-Kelishami, A., Ashrafizadeh, S.N., 2021. Combination of electrocoagulation and adsorption processes to remove methyl orange from aqueous solution. Environ. Technol. Innovat. 24, 102018.
Suhan, M.B.K., Mahtab, S.T., Aziz, W., Akter, S., Islam, M.S., 2021. Sudan black B dye degradation in aqueous solution by Fenton oxidation process: kinetics and cost analysis. Case Studies Chem.Environ. Eng. 4, 100126.
Suhan, M.B.K., Shuchi, S.B., Anis, A., Haque, Z., Islam, M.S., 2020. Comparative degradation study of remazol black B dye using electro-coagulation and electro-Fenton process: kinetics and cost analysis. Environ. Nanotechnol. Monit. Manag. 14, 100335.
Sun, S.P., Li, C.J., Sun, J.H., Shi, S.H., Fan, M.H., Zhou, Q., 2009. Decolorization of an azo dye Orange G in aqueous solution by Fenton oxidation process: effect of system parameters and kinetic study. J. Hazard Mater. 161 (2-3), 1052–1057.
Tavangar, T., Jalali, K., Shahmirzadi, M.A.A., Karimi, M., 2019. Toward real textile wastewater treatment: membrane fouling control and effective fractionation of dyes/inorganic salts using a hybrid electrocoagulation–nanofiltration process. Separ. Purif. Technol. 216, 115–125.
Tiwari, B., Sellamuthu, B., Ouarda, Y., Drogui, P., Tyagi, R.D., Buelna, G., 2017. Review on fate and mechanism of removal of pharmaceutical pollutants from wastewater using biological approach. Bioresour. Technol. 224, 1–12.
Turan, N.B., 2020. The application of hybrid electrocoagulation–electrooxidation system for the treatment of dairy wastewater using different electrode connections. Separ. Sci. Technol. 1–14.
Vidal, J., Villegas, L., Peralta-Hernandez, J.M., Salazar Gonzalez, R., 2016. Removal of Acid Black 194 dye from water by electrocoagulation with aluminum anode. J. Environ. Sci. Health, Part A A. 51 (4), 289–296.
Vilar, V.J., Pinho, L.X., Pintor, A.M., Boaventura, R.A., 2011. Treatment of textile wastewaters by solar-driven advanced oxidation processes. Sol. Energy 85 (9), 1927–1934.
Wang, A., Qu, J., Ru, J., Liu, H., Ge, J., 2005. Mineralization of an azo dye Acid Red 14 by electro-Fenton's reagent using an activated carbon fiber cathode. Dyes Pigments 65 (3), 227–233.
Wang, Y., Xia, G., Wu, C., Sun, J., Song, R., Huang, W., 2015. Porous chitosan doped with graphene oxide as highly effective adsorbent for methyl orange and amido black 10B. Carbohydr. Polym. 115, 686–693.
Wesley, M.J., Lerner, R.N., Kim, E.-S., Islam, M.S., Liu, Y., 2011. Biological fixed film. Water environment research. Lit. Rev. 83 (10), 1150–1186.
Wu, Z., Dong, J., Yao, Y., Yang, Y., Wei, F., 2021. Continuous flowing electrocoagulation reactor for efficient removal of azo dyes: kinetic and isotherm studies of adsorption. Environ. Technol. Innovat. 22, 101448.
Yan, S.C., Li, Z.S., Zou, Z.G., 2010. Photodegradation of rhodamine B and methyl orange over boron-doped g-C3N4 under visible light irradiation. Langmuir 26 (6), 3894–3901.
Yang, Z.H., Xu, H.Y., Zeng, G.M., Luo, Y.L., Yang, X., Huang, J., Wang, L.K., Song, P.P., 2015. The behavior of dissolution/passivation and the transformation of passive films during electrocoagulation: influences of initial pH, Cr (VI) concentration, and alternating pulsed current. Electrochim. Acta 153, 149–158.
Yaseen, D.A., Scholz, M., 2019. Impact of pH on the treatment of artificial textile wastewater containing azo dyes using pond systems. Int. J. Environ. Res. 13 (2), 367–385.
Zaied, B.K., Rashid, M., Nasrullah, M., Zularisam, A.W., Pant, D., Singh, L., 2020. A comprehensive review on contaminants removal from pharmaceutical wastewater by electrocoagulation process. Sci. Total Environ. 138095.
Zeboudji, B., Drouiche, N., Lounici, H., Mameri, N., Ghaffour, N., 2013. The influence of parameters affecting boron removal by electrocoagulation process. Separ. Sci. Technol. 48 (8), 1280–1288.
Zhang, Z., Xu, Y., Ma, X., Li, F., Liu, D., Chen, Z., Zhang, F., Dionysiou, D.D., 2012. Microwave degradation of methyl orange dye in aqueous solution in the presence of nano-TiO2-supported activated carbon (supported-TiO2/AC/MW). J. Hazard Mater. 209, 271–277.
Zhao, H., Zhang, G., Zhang, Q., 2014. MnO2/CeO2 for catalytic ultrasonic degradation of methyl orange. Ultrason. Sonochem. 21 (3), 991–996.
Zodi, S., Potier, O., Lapicque, F., Leclerc, J.P., 2009. Treatment of the textile wastewaters by electrocoagulation: effect of operating parameters on the sludge settling characteristics. Separ. Purif. Technol. 69 (1), 29–36.